Network pharmacology based investigation into the bioactive ingredients and molecular mechanisms of QingFeiPaiDu Decoction treating COVID-19

Yan Liu (2018101033@sdutcm.edu.cn)
Shandong University of Traditional Chinese Medicine https://orcid.org/0000-0002-3459-165X
Lewen Xiong
Shandong University of Traditional Chinese Medicine
YanYu Wang
Shandong University of Traditional Chinese Medicine
Mengxiong Luo
Shandong University of Traditional Chinese Medicine
Longfei Zhang
Shandong University of Traditional Chinese Medicine
Yongqing Zhang
Shandong University of Traditional Chinese Medicine

Research

Keywords: QingFeiPaiDu Decoction, COVID-19, Bioactive ingredients, Molecular mechanism, Network pharmacology

Posted Date: June 16th, 2020

DOI: https://doi.org/10.21203/rs.3.rs-34402/v1

Version of Record: A version of this preprint was published at Journal of Exploratory Research in Pharmacology on July 30th, 2021. See the published version at https://doi.org/10.14218/JERP.2021.00011.

Network pharmacology based investigation into the bioactive ingredients and molecular mechanisms of QingFeiPaiDu Decoction treating COVID-19

Yan Liu[1+] Lewen Xiong[1+] YanYu Wang[1] Mengxiong Luo[1] Longfei Zhang[1*] Yongqing Zhang[1*]

[1]School of Pharmacy, Shandong University of Traditional Chinese Medicine, Jinan 250355, China

*Corresponding authors. E-mail addresses: longfei_zhang@sdutcm.edu.cn (Longfei Zhang), zyq622003@126.com (Yongqing Zhang).

[+]Yan Liu, and Lewen Xiong have equal contributions to this study.

Abstract Background: To study the QingFeiPaiDu Decoction (QFPDD) in the treatment of Corona Virus Disease 2019 (COVID-19) bioactive ingredient and its potential mechanism. **Methods:** Combined with the clinical symptoms of COVID-19 patients, a "component-target-disease" network model was constructed based on the network pharmacology method, and potential active components, targets and molecular mechanisms of QFPDD for COVID-19 were screened out through topology parameter analysis. **Results:** We collected 376 active ingredients of QFPDD from the database, and 18833 potential anti-severe acute respiratory syndrome coronavirus 2 (SARS-CoV-2) targets were analyzed and screened. The principal targets involved PIK3CA, PIK3R1, APP, SRC, MAPK1, MAPK3, AKT1, HSP90AA1, EP300, CDK1, etc. We obtained 574 GO entries by Gene Ontology enrichment analysis and obtained 214 signal pathways with $P<0.05$ by KEGG (Kyoto Encyclopedia of Genes and Genomes) pathway analysis. Among them, the antiviral biological processes of QFPDD included a cellular response to nitrogen compound, protein kinase activity, membrane raft, etc. Pathways involved in the regulation include Pathways in cancer, Endocrine resistance, PI3K-Akt signaling pathway, Proteoglycans in cancer, etc. Molecular docking results showed that the core ingredients of QFPDD have a better affinity to the 2019-nCoV 3-chymotrypsin-like cysteine protease (3CLpro) and

angiotensin-converting enzyme 2 (ACE2). **Conclusions:** Through network pharmacology research and molecular docking verification, this paper preliminarily explored the potential molecular mechanism and relevant active ingredients of QFPDD playing an anti-SARS-CoV-2 role, providing a reference for the further development and utilization of QFPDD and the development of new specific antiviral drugs.

Keywords QingFeiPaiDu Decoction; COVID-19; Bioactive ingredients; Molecular mechanism; Network pharmacology

1. Background

WHO declared Corona Virus Disease 2019(COVID-19) a global pandemic on 14 March 2020. This disease is caused by severe acute respiratory syndrome coronavirus 2 (SARS-COV-2) infection, which rapidly affects the whole country and even some foreign countries due to its high pathogenicity and strong infectiousness, and has a serious impact on people's life safety, national economic development and social stability. At present, most of the therapeutic drugs and methods used in clinical practice are derived from the experience in the treatment of SARS and MERS [1-2]. No specific therapeutic drugs and treatment plans have been found, so it is urgent to find and develop drugs for the treatment of COVID-19.

The epidemic in China is now well under control and nearing its end. Many countries and international organizations have recognized the positive and effective measures China has taken. Among them, traditional Chinese medicine plays a decisive role in controlling the disease with its unique advantages. COVID-19 belongs to the category of "epidemic disease" in traditional Chinese medicine because the disease suffered from "epidemic plagues," the cause of the disease was considered to be closely related to the deficiency of healthy qi of the patients, so the infected people were mostly the elderly or patients with complications. The patient's healthy qi is not reliable, the external pathogenic qi invades, struggling between healthy qi and

pathogenic qi, consumes the body's healthy qi, and hinders the body's zang-fu function regular operation, causes the disease occurrence and the development. QingFeiPaiDu Decoction (QFPDD) is aimed at the etiology, the pathogenesis of COVID-19, according to the six-meridian syndrome differentiation identification, composed of four classic prescriptions, namely Ephedra, Apricot Kernel, Gypsum, and Licorice Decoction, Belamcanda and Ephedra Decoction, Minor Bupleurum Decoction, and Powder of Five Ingredients with Poria, derived from Treatise on Cold Damage and Miscellaneous Diseases, used in the treatment of patients with light, regular and substantial, rational use of critically ill patients combined with the actual situation. QFPDD is quick, efficient, safe and low-cost, and is the only universal prescription included in the COVID-19 guidelines, which contains 21 traditional Chinese medicines with complicated ingredients, and its clinical efficacy is the result of multi-ingredient, multi-target, and multi-pathway exerting all-round and overall regulation on the body. To develop anti-SARS-CoV-2 drugs, we used network pharmacological means [3], combined with the main clinical symptoms of COVID-19 patients, to explore the active ingredients and potential molecular mechanism of QFPDD in the treatment of COVID-19. The research workflow is shown in Fig. 1.

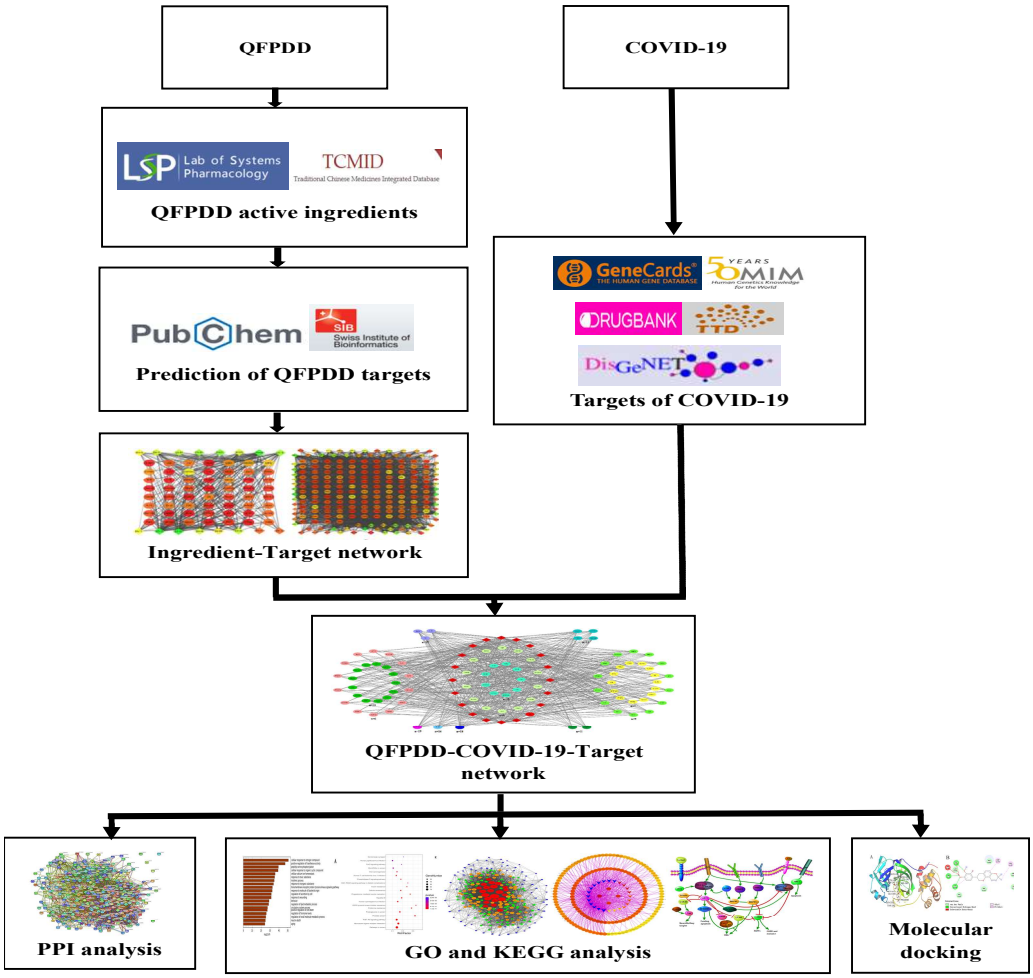

Fig.1 The workflow diagram of QFPDD in the treatment of COVID-19

2. Materials and methods

2.1 Collection of active ingredients of QFPDD

Using Traditional Chinese Medicine Systems Pharmacology [4] (TCMSP, http://tcmspw.com/index.php) and Traditional Chinese Medicines Integrated Database [5] (TCMID, http://119.3.41.228:8000/tcmid/search), the active ingredients of QFPDD were screened with oral bioavailability (OB)≥30% and drug-likeness [6-7] (DL)≥0.18 as the criteria. As Gypsum Fibrosum belongs to mineral medicine, its composition is relatively simple, so these criteria do not screen it.

2.2 Prediction of active ingredient targets of QFPDD

Using the PubChem database (https://pubchem.ncbi.nlm.nih.gov/) [8] and SwissTargetPrediction database (http://www.swisstargetprediction.ch) [9] get active ingredient prediction targets (eliminate P=0 and screen the target of P>median).

2.3 Screening of main active ingredients and targets of QFPDD

Cytoscape software (version 3.7.2) was used to construct the ingredient-target network diagram [10-11], and the Cytoscape tool was used to calculate the network topology parameters. The main active ingredients and targets of QFPDD were screened according to the average degree of freedom and the maximum degree of freedom [12].

2.4 Collection of major symptom targets of COVID-19

The main symptoms of COVID-19 patients were fever, cough, fatigue, etc. In GeneCards database (https://www.genecards.org) [13], TTD database (http://db.idrblab.net/ttd) [14], DrugBank database (https://www.drugbank.ca) [15], DisGeNet database (https://www.disgenet.org/search) [16] and OMIM database (https://omim.org) [17] search for corresponding disease targets.

2.5 Construction and analysis of "QFPDD-COVID-19-Target" network

The main active ingredient targets and disease targets were established in pairs to obtain the potential targets of QFPDD in the treatment of COVID-19. The obtained data were imported into Cytoscape software (version 3.7.2) for visual processing to construct the "QFPDD-COVID-19-Target" network [11,18]. Topological parameters of the constructed network graph were analyzed to explore the interaction of different traditional Chinese medicines in QFPDD in the treatment of COVID-19.

2.6 Construction and analysis of protein-protein interaction

The potential targets of QFPDD in the treatment of COVID-19 were imported into the String database (https://string-db.org)[19-21], and the protein-protein interaction (PPI) network of potential targets was obtained, and the interaction targets with confidence score≥0.9 were screened. For further analysis of the interaction between target and screening key targets, the income data import Cytoscape software version (3.7.2) topology parameters analysis, including each node degree, betweenness centrality, closeness centrality, and average shortest path length, with their average as the filter to filter the key targets.

2.7 GO enrichment analysis and KEGG pathway analysis

Through Metascape website (http://metascape.org) [22] to get QFPDD potential

targets for the treatment of COVID-19 to GO (Gene Ontology) enrichment analysis, at the same time with DAVID website (https://david.ncifcrf.gov/) [23] and KEGG database (Kyoko Encyclopedia of Genes and Genomes) [24-25] signaling pathway enrichment analysis. The potential targets were input, and the species were restricted to be human. The analysis results were screened with P≤0.05 as the index.

2.8 Molecular docking

From the RSCB database(https://www.rcsb.org/), downloading the 3D structure of the SARS-CoV-2 3-chymotrypsin-like cysteine protease (3CLpro) (PDB ID:6LU7) and angiotensin-converting enzyme 2 (ACE2)(PDB ID:1R42). Original receptor proteins are extracted using Pymol1.7.2.1 software, removal of water molecules, other ligands, and residue. Using AutoDock Tools1.5.6 software for hydrogenation, merge nonpolar hydrogen operation and saving in PDBQT format. 2D or 3D structures of ligand compounds were downloaded from the PubChem database. The energy of ligand compounds was minimized and saved in mol2 format by Chemoffice2016 software. Hydrogenation and other optimization processes were performed by AutoDock Tools1.5.6 software. All the flexible bonds of ligand compounds could be rotated by default. The grid box of molecular docking was set as all the surrounding residues centered on the primary ligands of receptor proteins. The Autodock Vina1.1.2 and Python script were used for molecular docking, and the sequence was sorted according to the optimal binding energy (affinity) of each ligand compound.

3. Results

3.1 Active ingredients of QFPDD

There are 376 ingredients of OB≥30%, DL≥0.18 in 20 traditional Chinese medicines and Gypsum Fibrosum of QFPDD, including Ephedrae Herba (EH) contains 23, Glycyrrhizae Radix et Rhizoma (GRR) contains 92, Armeniacae by Amarum (ASA) contains 19, Gypsum Fibrosum (GF) contains 1, Cinnamomi Ramulus (CR) contains 7, Alismatis Rhizoma (AR) contains 10, Polyporus (POL) contains 11, Atractylodis Macrocephalae Rhizoma (AMR) contains 7, Poria (POR) contains 15, Bupleuri Radix (BUP) contains 17, Scutellariae Radix (SR) contains 36,

Pinelliae Rhizoma (PR) contains 13, Zingiberis Rhizoma Recens (ZRR) contains 5, Asteris Radix et Rhizoma (AST) contains 19, Farfarae Flos (FF) contains 22, Belamcandae Rhizoma (BR) contains 17, Asari Radix et Rhizoma (ARR) contains 8, Dioscoreae Rhizoma (DR) contains 16, Aurantii Fructus Immaturus (AFI) contains 22, Citri Reticulatae Pericarpium (CRP) contains 5, and Pogostemonis Herba (PH) contains 11. Details are listed in supplementary document 1 (sheet 1). Because Asteris Radix et Rhizoma and Asari Radix et Rhizoma have the same Latin initials, to distinguish the two traditional Chinese medicines, the first three letters of the first word of Asteris Radix et Rhizoma were taken to represent the traditional Chinese medicine. Bupleuri Radix, Poria and Polyporus, the abbreviation of the situation with Asteris Radix et Rhizoma.

3.2 Active ingredient targets of QFPDD

A total of 18833 targets were found for 376 active ingredients in QFPDD (except for the targets of Gypsum Fibrosum, and some active ingredients were not found at present). Detailed target information of 20 active ingredients of traditional Chinese medicine was shown in supplementary document 2.

3.3 Main active ingredients and targets of QFPDD

Although many ingredients of QFPDD are helpful in the treatment of COVID-19, the study of the main ingredients of TCM compounds is an effective way to elucidate the mechanism of its pharmacological action. In this study, network pharmacology was used to explore its core ingredients. We constructed the ingredient-target network (Fig.2) for these 20 traditional Chinese medicines, and refer to supplementary document 1 (sheet 2) for the abbreviation of related ingredients. According to the results of the ingredient-target network diagram of 20 Chinese medicines, 39 core ingredients and corresponding targets of 20 Chinese medicines were screened from the ingredient-target perspective, as shown in Table 1

Table 1 Main active ingredients and targets of 20 traditional Chinese medicines

Chinese name	Latin name	Number of major ingredients	Core ingredients	Core targets
麻黄	Ephedrae Herba	16	diosmetin (EH-10) genkwanin (EH-14) kaempferol (EH-04)	CYP19A1

炙甘草	Glycyrrhizae Radix et Rhizoma	75	3'-Methoxyglabridin (GRR-63) glypallichalcone (GRR-26) glyasperin B (GRR-18)	CYP19A1 PTPN1 ESR2 ESR1
杏仁	Armeniacae Semen Amarum	17	gondoic acid (ASA-13) spinasterol (ASA-08)	ESR1 ESR2 HSD11B2
桂枝	Cinnamomi Ramulus	3	peroxyergosterol (CR-03) sitosterol (CR-02) beta-sitosterol (CR-01)	CDC25A NOS2 NR1H2 GLRA1 DHCR7 CDC25B
泽泻	Alismatis Rhizoma	9	alisol,b,23-acetate (AR-04) [(1S,3R)-1-[(2R)-3,3-dimethyloxiran-2-yl]-3-[(5R,8S,9S,10S,11S,14R)-11-hydroxy-4,4,8,10,14-pentamethyl-3-oxo-1,2,5,6,7,9,11,12,15,16-decahydrocyclopenta[a]phenanthren-17-yl]butyl] acetate (AR-08) alisol B monoacetate (AR-03)	AR CES2 CYP17A1 HMGCR HSD11B1 PTPN1
猪苓	Polyporus	8	(22e,24r)-ergosta-6-en-3beta,5alpha,6beta-triol (POL-03) Cerevisterol (POL-01)	AR
白术	Atractylodis Macrocephalae Rhizoma	3	α-Amyrin (AMR-01) (3S,8S,9S,10R,13R,14S,17R)-10,13-dimethyl-17-[(2R,5S)-5-propan-2-yloctan-2-yl]-2,3,4,7,8,9,11,12,14,15,16,17-dodecahydro-1H-cyclopenta[a]phenanthren-3-ol (AMR-02)	CYP19A1 AR CDC25A
茯苓	Poria	14	3beta-Hydroxy-24-methylene-8-lanostene-21-oic acid (POR-09) trametenolic acid (POR-02) dehydroeburicoic acid (POR-14)	SHBG PTPN1 HSD11B1
柴胡	Bupleuri Radix	13	3,5,6,7-tetramethoxy-2-(3,4,5-trimethoxyphenyl)chromone(BUP-07) quercetin (BUP-01) areapillin (BUP-08)	CYP19A1
黄芩	Scutellariae Radix	32	5,8,2'-Trihydroxy-7-methoxyflavone (SR-13) moslosooflavone (SR-28)	ESR2
姜半夏	Pinelliae Rhizoma	10	beta-sitosterol (PR-01) gondoic acid (PR-08)	ACHE CYP19A1 ESR2 AR
生姜	Zingiberis Rhizoma Recens	4	beta-sitosterol (ZRR-01) poriferast-5-en-3beta-ol (ZRR-03) stigmasterol (ZRR-02)	ACHE SLC6A2 BCHE SLC6A4 CHRM2 CDC25A
紫菀	Asteris Radix et Rhizoma	14	quercetin (AST-02) galangin (AST-06)	CDC25B ACHE CYP19A1
冬花	Farfarae Flos	8	quercetin (FF-01) femara (FF-08) tussilagolactone (FF-06)	CDK1
射干	Belamcandae Rhizoma	15	epianhydrobelachinal (BR-10) anhydrobelachinal (BR-06)	CYP19A1 CA2 CDK1
细辛	Asari Radix et Rhizoma	8	4,9-dimethoxy-1-vinyl-$b-carboline (ARR-07)	CDK2 CYP19A1 CA12
山药	Dioscoreae Rhizoma	10	denudatin B (DR-01) kadsurenone (DR-02)	CYP19A1 PTPN1 AR
枳实	Aurantii Fructus Immaturus	20	sinensetin (AFI-03)	ADORA1
陈皮	Citri Reticulatae Pericarpium	5	5,7-dihydroxy-2-(3-hydroxy-4-methoxyphenyl)chroman-4-one (CRP-03)	ABCG2 ADORA1

			naringenin (CRP-02)	ADORA3 CYP19A1 CYP1B1
藿香	Pogostemonis Herba	7	quercetin (PH-01)	ADORA1

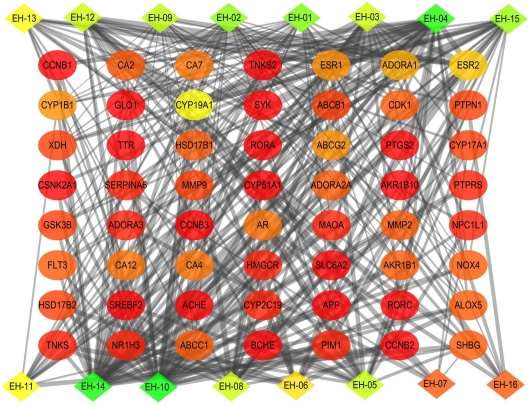

A

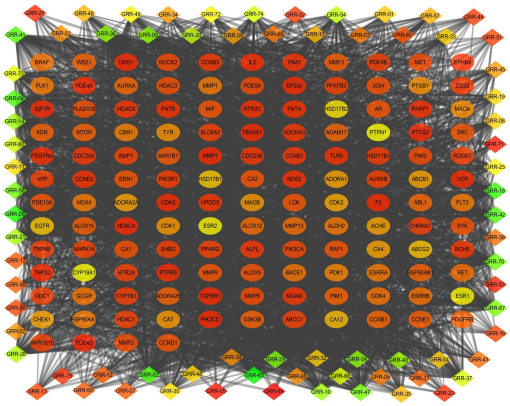

B

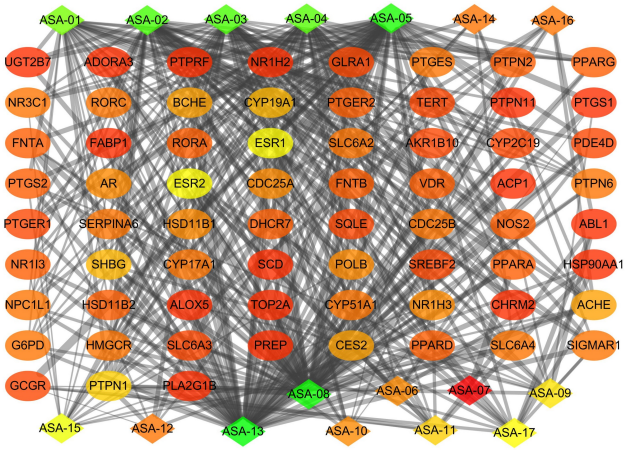

C

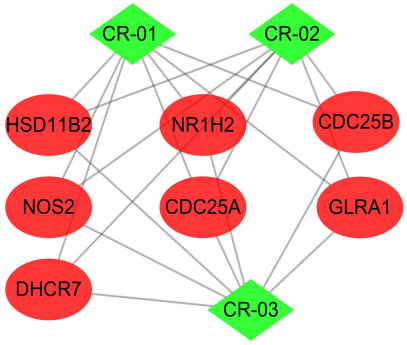

D

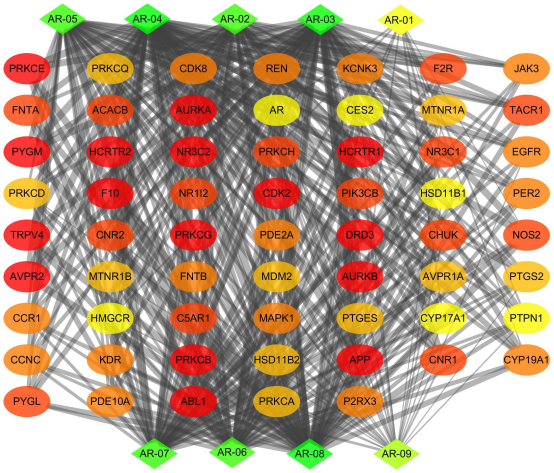

E

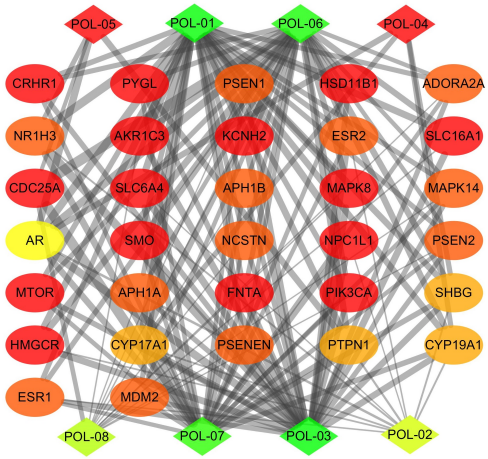

F

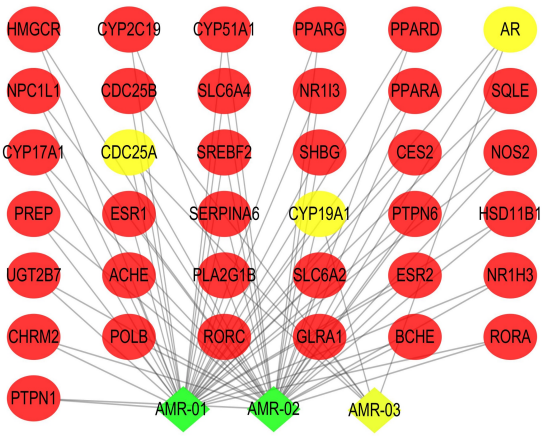
HMGCR
CYP2C19
CYP51A1
PPARG
PPARD
AR
NPC1L1
CDC25B
SLC6A4
NR1I3
PPARA
SQLE
CYP17A1
CDC25A
SREBF2
SHBG
CES2
NOS2
PREP
ESR1
SERPINA6
CYP19A1
PTPN6
HSD11B1
UGT2B7
ACHE
PLA2G1B
SLC6A2
ESR2
NR1H3
CHRM2
POLB
RORC
GLRA1
BCHE
RORA
PTPN1
AMR-01
AMR-02
AMR-03

G

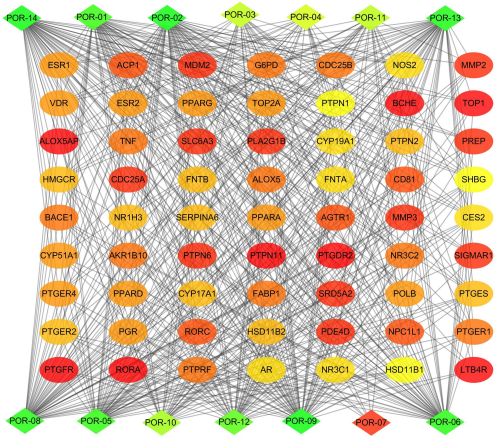

H

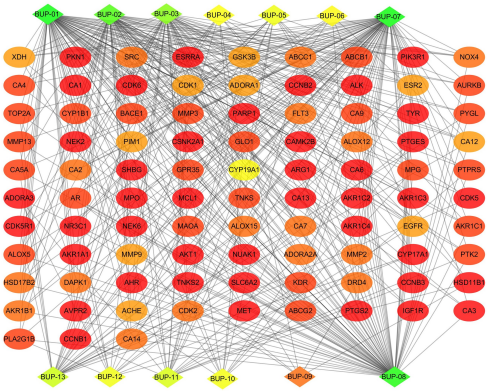

I

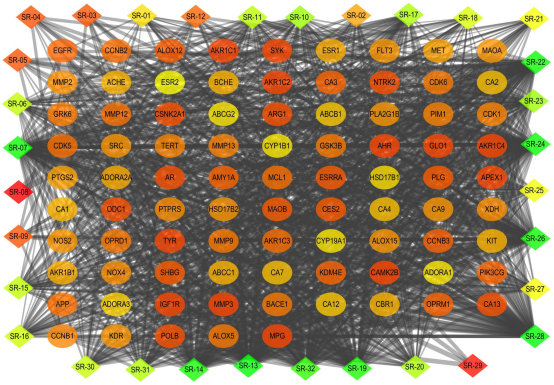

J

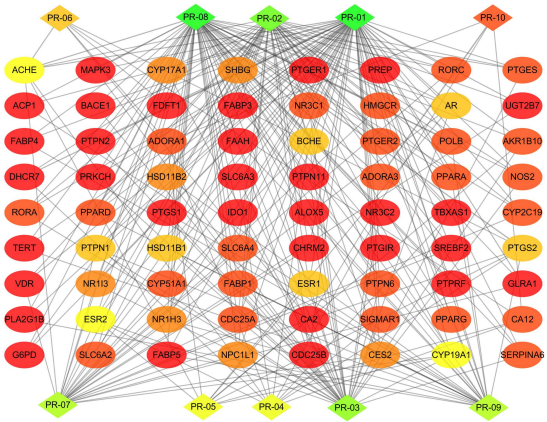

K

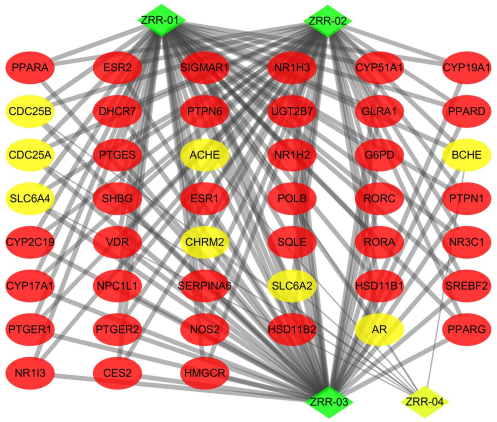

L

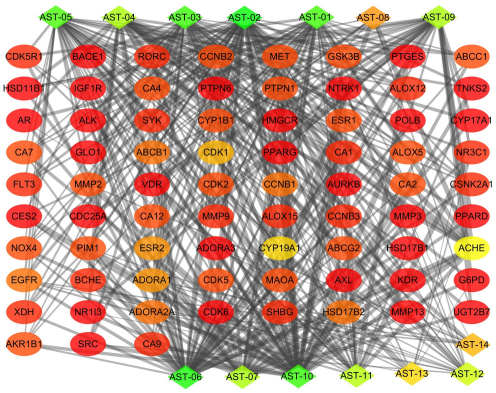

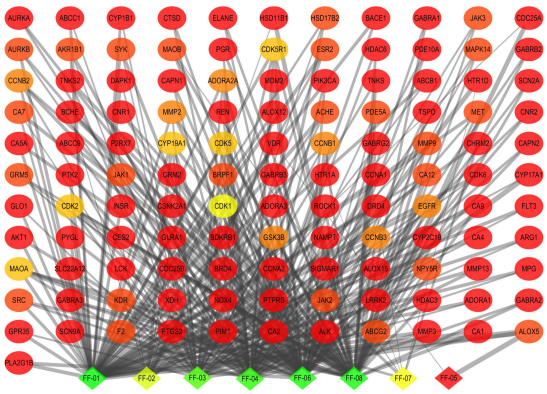

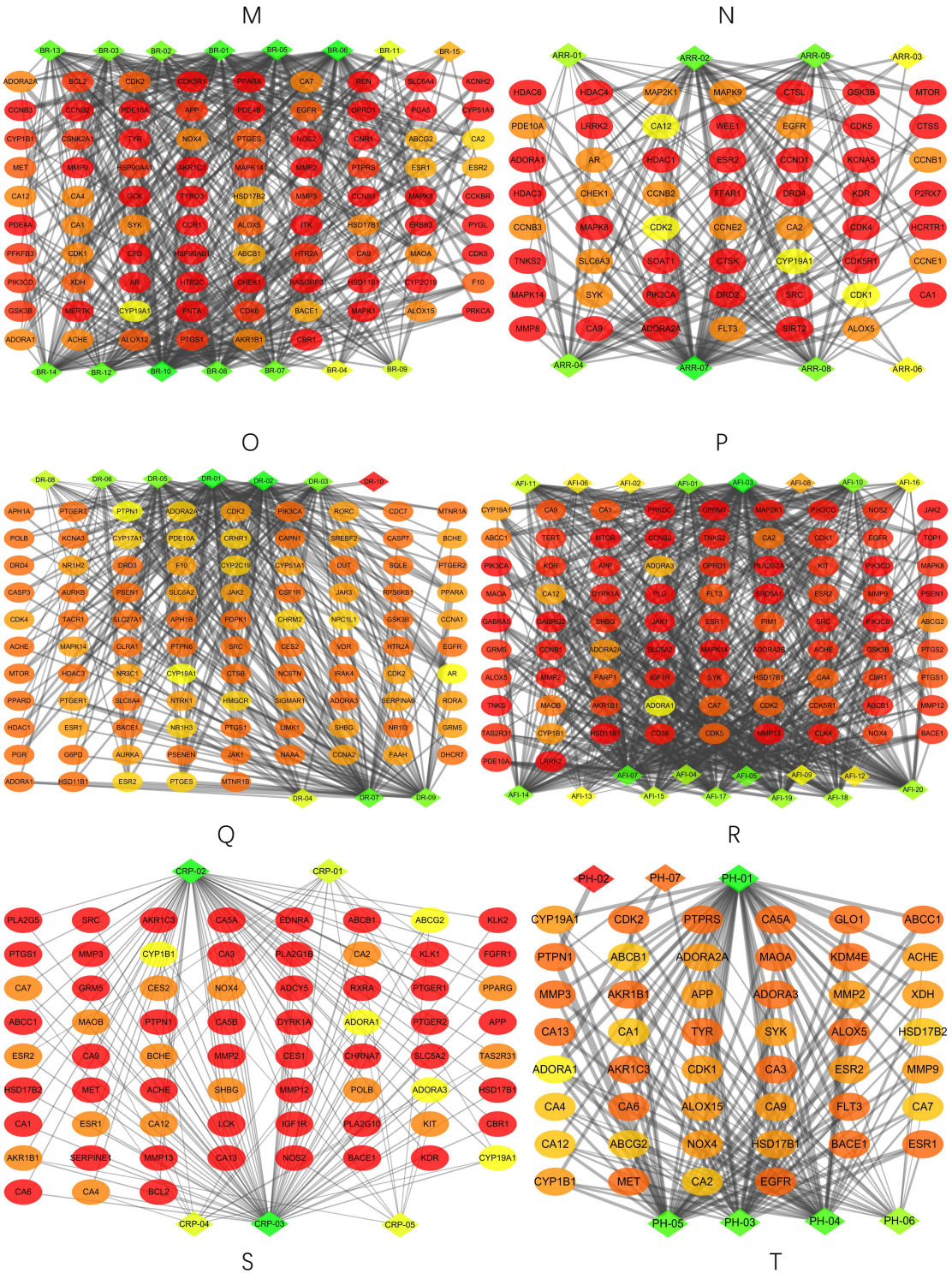

Fig.2 Ingredient-Target network

(A)EH, (B)GRR, (C)ASA, (D)CR, (E)AR, (F)POL, (G)AMR,(H)POR,(I)BUP, (J)SR, (K)PR, (L)ZRR, (M)AST, (N)FF, (O)BR, (P)ARR, (Q)DR, (R)AFI, (S)CRP, (T)PH (The rhomboid node represents the ingredient, and the circular node represents the target. The color of the node is represented in ascending order of

degrees of freedom from red to yellow to green, and the size of Edge betweenness denotes the thickness of the line.)

3.4 Targets of significant symptoms of COVID-19

To explore the molecular mechanism of the drug's effect, 9,624 targets for fever, cough, and fatigue were collected from the database, details of which are listed in supplement 1(sheet 3).

3.5 "QFPDD-COVID-19-Target" Network

Different Chinese medicines can act on the same target when treating COVID-19, play a synergistic role, and enhance the efficacy. Take a network of traditional Chinese medicines and targets with six or more of the mutual target medicines, as shown in Fig.3. Among these targets, 19 kinds of Chinese traditional medicines are acting on the same target CYP19A1, 18 Chinese traditional medicines acting on the same target ESR2, 15 Chinese traditional medicines have three common targets, 14 Chinese traditional medicines acting on the same target SHBG. There are four were mutual targets of 13 kinds of Chinese medicines, nine were common targets of 12 Chinese medicines, two were common targets of 11 Chinese medicines, 13 were common targets of 10 Chinese medicines, 14 were common targets of nine Chinese medicines, 14 were common targets of eight kinds of traditional Chinese medicine, 14 were common targets of seven kinds of traditional Chinese medicine, and 14 were common targets of six kinds of traditional Chinese medicine, which fully illustrates the "multi-ingredient-multi-target" of traditional Chinese medicine Point feature.

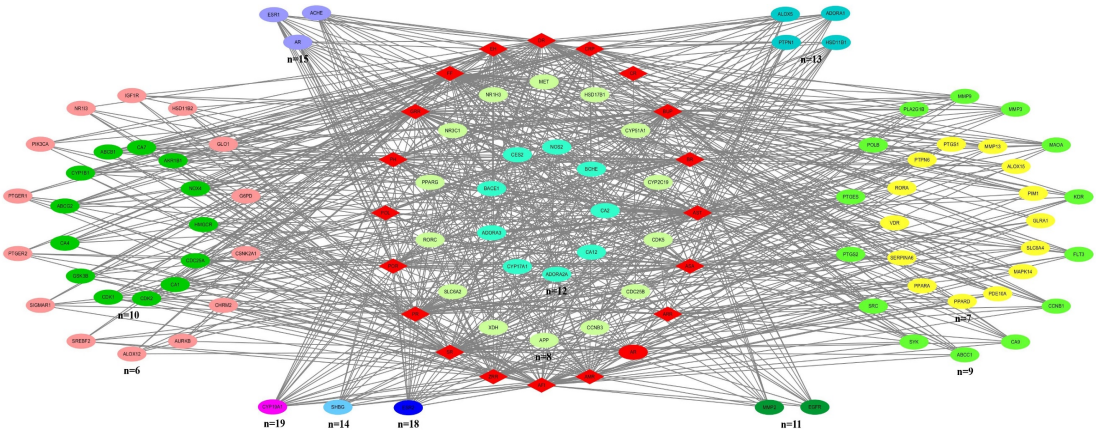

Fig.3 QFPDD-COVID-19-Target Network

(the rhomboid node represents the traditional Chinese medicine, the circular node represents the target, and n represents the number of types of targets distributed in the same circle acting on the same amount of traditional Chinese medicine.)

3.6 PPI network

The potential targets of QFPDD in the treatment of COVID-19 were analyzed through the String database, and the PPI network of protein interactions was obtained (Fig.4).

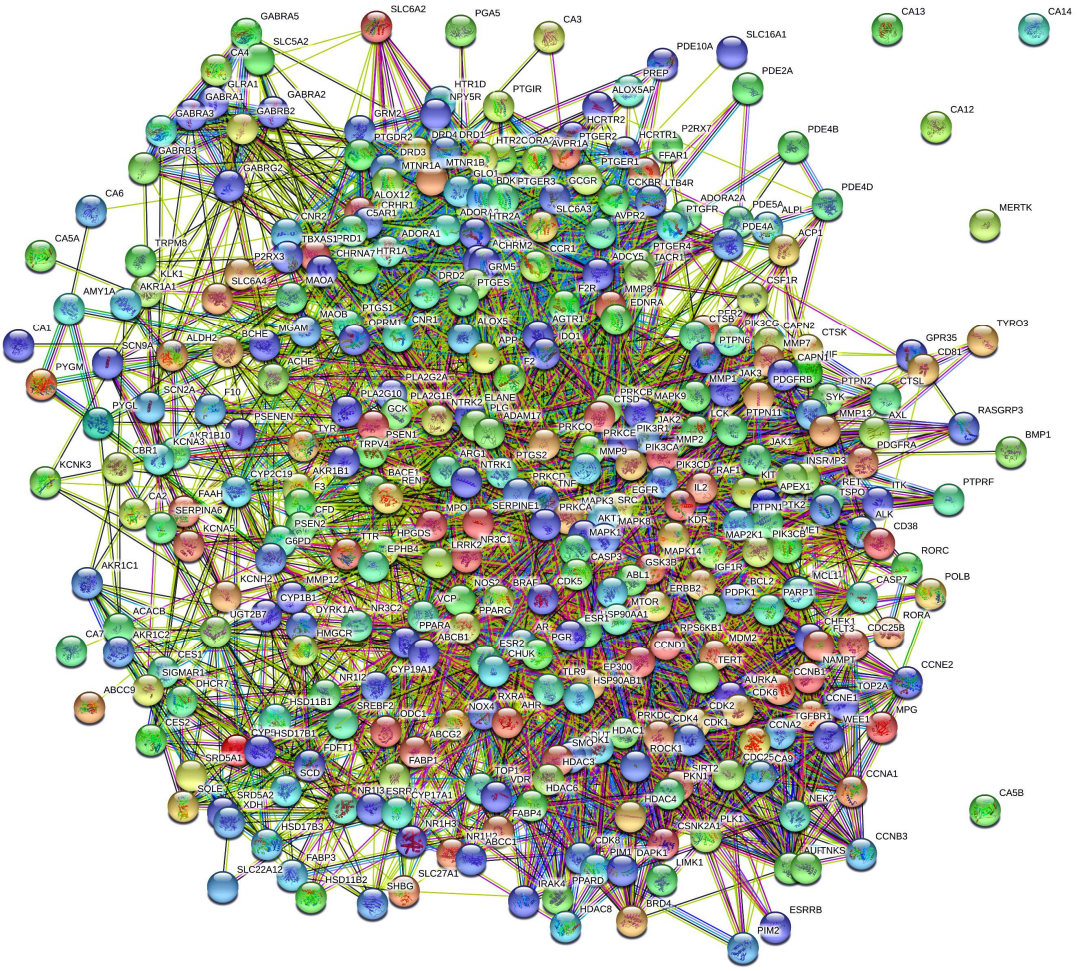

Fig.4 Protein-protein interaction (PPI) network of potential targets of COVID-19 treated with QFPDD

Through the calculation of the degree of each node, betweenness centrality, closeness centrality, and average shortest path length selected 24 key targets, the target information according to the degree of descending order, are shown in Table 2.

Table2 Topological analysis of QFPDD-COVID-19-Target network

Target name	Abbreviation	Uniprot ID	ASPL	BC	CC	Degree
Phosphatidylinositol-4,5-bisphosphate 3-kinase catalytic subunit alpha	PIK3CA	P42336	2.189	0.098	0.457	66
Phosphoinositide-3-kinase regulatory subunit 1	PIK3R1	P27986	2.205	0.086	0.454	62
Amyloid beta precursor protein	APP	P05067	2.358	0.166	0.424	55
SRC proto-oncogene, non-receptor tyrosine kinase	SRC	P12931	2.280	0.053	0.439	49
mitogen-activated protein kinase 1	MAPK1	P28482	2.130	0.084	0.470	47
mitogen-activated protein kinase 3	MAPK3	P27361	2.224	0.042	0.450	43
AKT serine/threonine kinase 1	AKT1	P31749	2.268	0.063	0.441	40
heat shock protein 90 alpha family class A member 1	HSP90AA1	P07900	2.311	0.065	0.433	38
E1A binding protein p300	EP300	Q09472	2.453	0.065	0.408	34
cyclin dependent kinase 1	CDK1	P06493	2.614	0.033	0.382	30
Janus kinase 2	JAK2	O60674	2.512	0.017	0.398	30
epidermal growth factor receptor	EGFR	P00533	2.370	0.041	0.422	29
Thrombin	F2	P00734	2.508	0.033	0.399	28
mitogen-activated protein kinase 8	MAPK8	P45983	2.283	0.045	0.438	28
retinoid X receptor alpha	RXRA	P19793	2.500	0.072	0.400	27
estrogen receptor 1	ESR1	P03372	2.382	0.090	0.420	27
protein kinase C delta	PRKCD	Q05655	2.563	0.015	0.390	23
protein tyrosine kinase 2	PTK2	Q05397	2.618	0.012	0.382	22
ribosomal protein S6 kinase B1	RPS6KB1	P23443	2.480	0.012	0.403	21
mitogen-activated protein kinase 14	MAPK14	Q16539	2.567	0.012	0.390	21
nuclear receptor subfamily 3 group C member 1	NR3C1	P04150	2.430	0.022	0.412	21
protein kinase C epsilon	PRKCE	Q02156	2.594	0.015	0.385	17
cyclin dependent kinase 5	CDK5	Q00535	2.634	0.028	0.380	17
peroxisome proliferator activated receptor alpha	PPARA	Q07869	2.587	0.031	0.387	15

Note: ASPL: Average Shortest Path Length; BC: Betweenness Centrality; CC: Closeness Centrality.

3.7 GO enrichment analysis and KEGG pathway analysis results

Metascape website was used to conduct GO enrichment analysis on the potential targets of QFPDD in the treatment of COVID-19, and a total of 574 GO entries with $P<0.05$, a minimum count of 3 and an enrichment factor>1.5 (the enrichment factor is the ratio between the observed counts and the counts expected by chance) were obtained, including 353 entries of Biological process, 112 entries of Molecular function, and 109 entries of Cell composition. The biological process enrichment of the items in the top 20 of each category and the lung related genes is shown in Fig.5(A), (B), (C), and (D). 214 signaling pathways with $P<0.05$ were obtained through KEGG pathway analysis. PI3K-Akt signaling pathway, JAK-STAT signaling pathway, AMPK signaling pathway, NOD-like receptor signaling pathway, NF-κB signaling pathway, Notch signaling pathway, TGF-β signaling pathway, HIF-1 Signaling pathways [26-37] have been reported to be associated with pneumonia. The top 20 pathways of all signaling pathways are shown in Fig.4(E). One hundred

ninety-six signaling pathways with P<0.01 were screened, and a total of 262 genes were annotated to these pathways. The correlation map of these genes was plotted to obtain the correlation of genes on different pathways, as shown in Fig.6. The degree value of the node in the figure reflects the degree of association between genes and disease treatment, and the node in front of the degree value may be the target gene we are looking for. The 24 critical targets screened by network analysis all have high degree values. These genes are the critical target genes of QFPDD in the treatment of COVID-19. According to the statistics of the occurrence of 24 critical targets in 196 signaling pathways, it was found that they were involved in the transduction of 156 signaling pathways, as shown in Fig.7, including Pathways in cancer, Endocrine resistance, PI3K-Akt signaling pathway, Proteoglycans in cancer, and Rap1 signaling pathway. Rap1 signaling pathway has been found to play an essential role in the pathogenesis of acute lung injury/acute respiratory distress syndrome (ALI/ARDS), and the regulation of the Rap1 signaling pathway may become a new target for the treatment of ALI/ARDS [38]. The schematic diagram of 24 critical targets involved in the treatment of COVID-19 is shown in Fig.8.

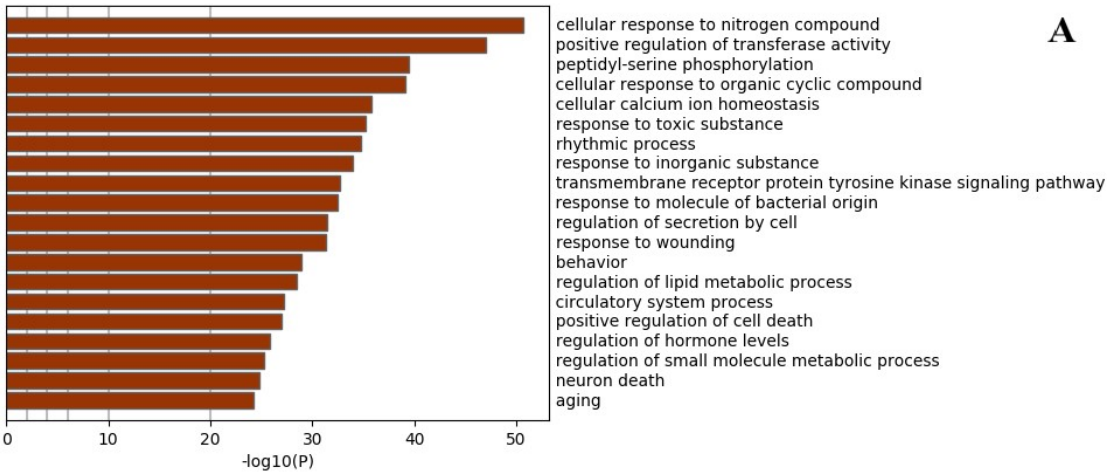

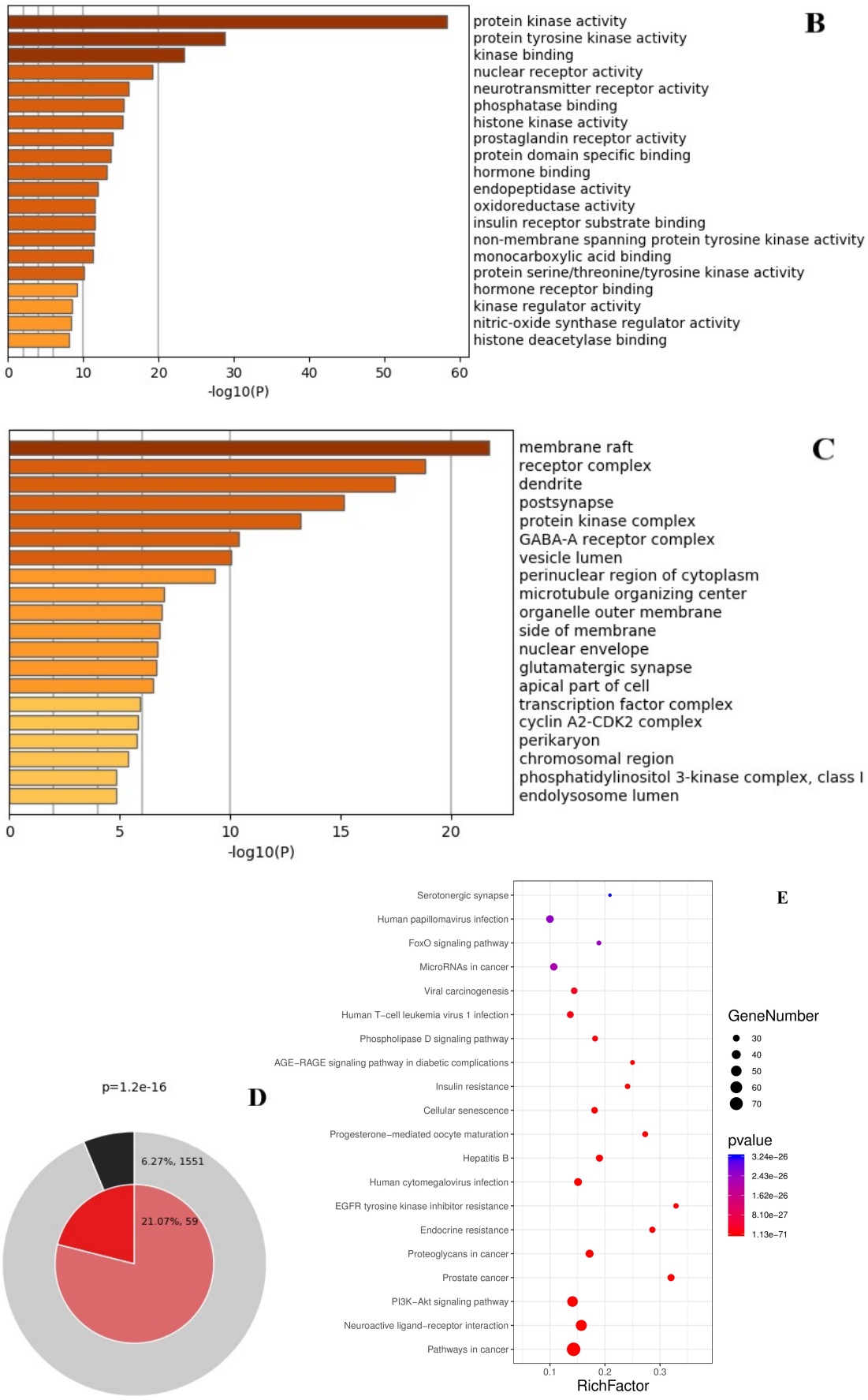

Fig.5 GO enrichment analysis and KEGG pathway analysis of potential targets in

QFPDD (A) Enrichment analysis of biological processes (B) Enrichment analysis of molecular functions (C) Enrichment analysis of cell ingredients. The bars of each enrichment item were colored with p values. (D) Biological process enrichment of genes matching membership term: lung. The outer pie shows the number and the percentage of genes in the background that is associated with the membership (in black); the inner pie shows the number and the percentage of genes in the individual input gene list that is associated with the membership. The p-value indicates whether the membership is statistically significantly enriched in the list. (E) KEGG pathway analysis. The size of the bubble in the figure represents the gene count of this line, and the color from cold to hot represents the P-value from large to small.

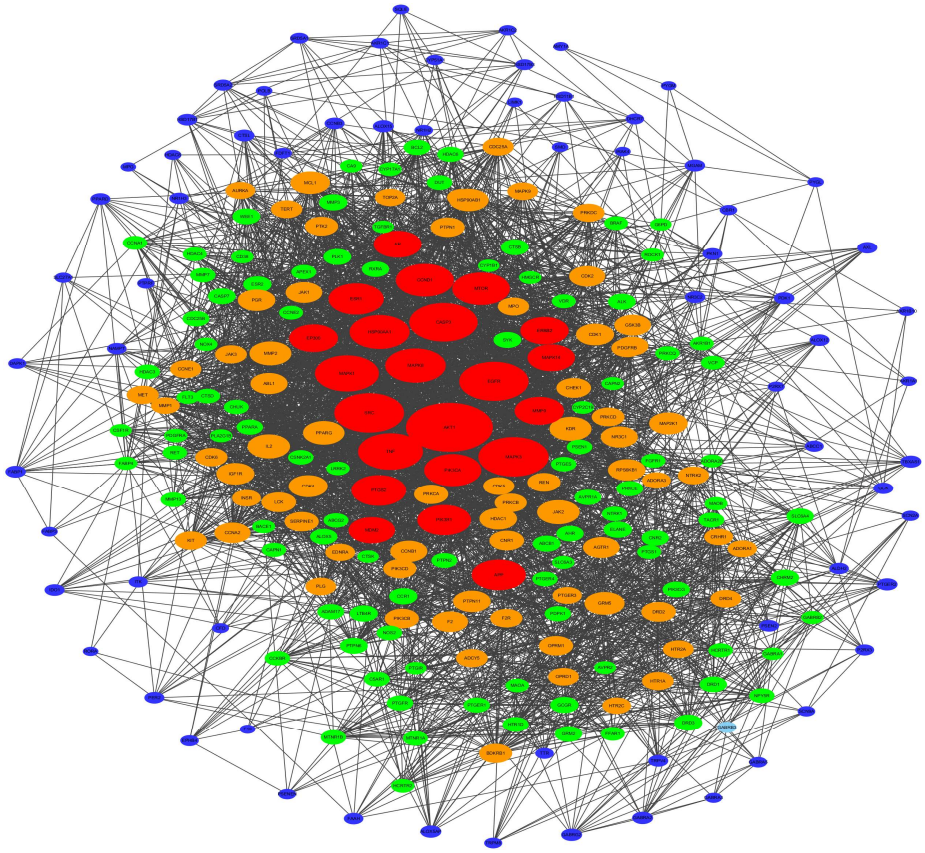

Fig.6 gene associations on different signaling pathways (the size of nodes in the figure represents the size of degree)

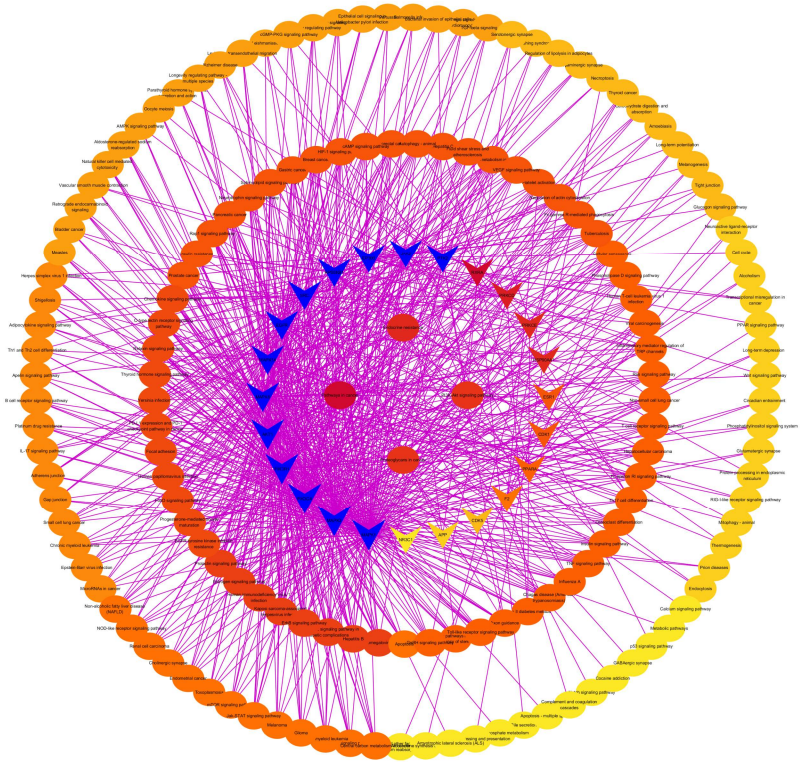

Fig.7 Target-Signal pathway diagram (the circular node represents the signal pathway in which 24 key targets participate, and the v-shaped node represents 24 key targets. The color of the node is represented by ascending order of degree from yellow to orange to red to blue)

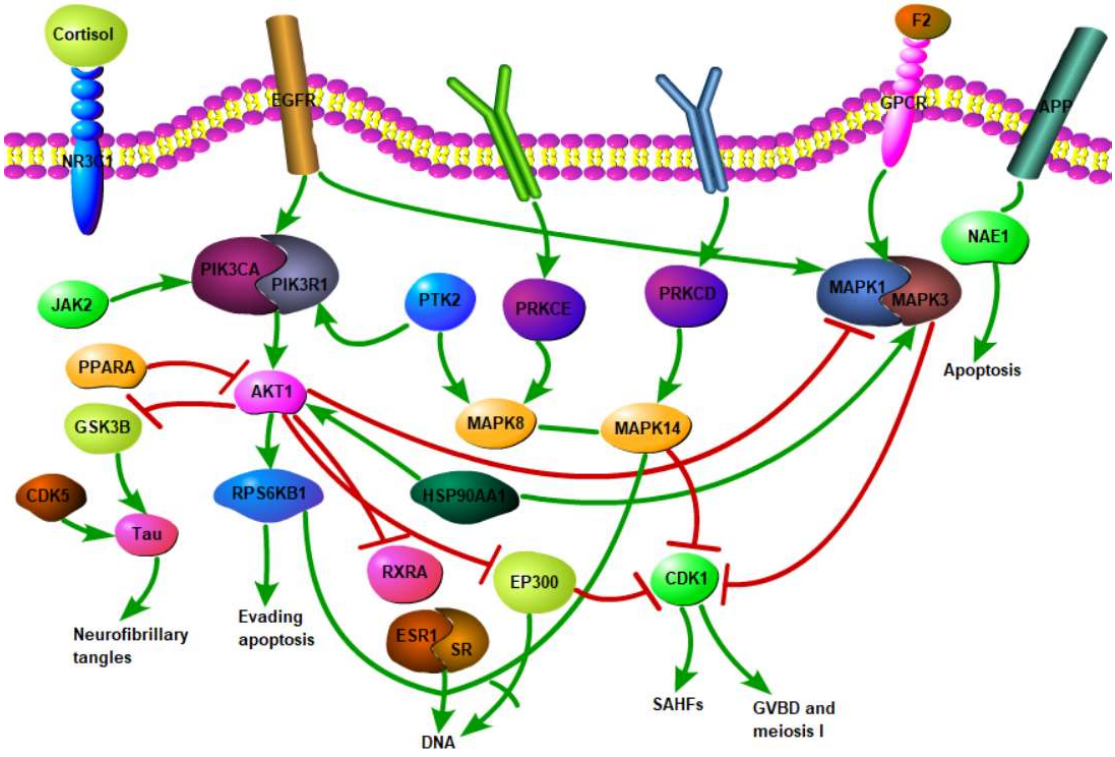

Fig.8 Schematic diagram of 24 critical targets involved in the treatment of COVID-19 signaling pathway (all targets are expressed by gene name)

3.7 Molecular docking results

Three hundred seventy-five main active ingredients of 20 traditional Chinese medicines (except Gypsum Fibrosum) in QFPDD were selected and screened for molecular docking with the ACE2 and 2019-nCoV 3CLpro. If the binding energy is less than 0, it indicates that ligand compounds can spontaneously bind to receptor proteins. The lower the binding energy is, the higher the possibility of its action is. The docking results showed that the binding energies of 375 main active ingredients were all<0(except taraxanthin and delphinidin). The 39 core ingredients screened by the ingredient-target network under 3.3 all have good affinity with 3CLpro and ACE2 proteins, and their binding energies are all less than -3.9. The docking results of each core ingredient with 3CLpro and ACE2 are shown in Table 3. To further analyze the interaction between ingredient and protein, 2D and 3D molecular docking diagrams of interaction between the ingredient and 3CLpro and ACE2 were constructed, respectively. The molecular docking diagrams of the ingredient with the best results were selected, as shown in Fig.9. Due to hydrophobic Pi-Alkyl, 3'-Methoxyglabridin parent nucleus mainly binds to amino acid residues CYS145, MET165, and PRO168 of 3CLpro. Meanwhile, hydrogen bonds are formed between phenolic hydroxyl on parent nucleus and amino acid residues GLY143, LEU141, and CYS145. Due to hydrophobic Pi-Alkyl, Alisol,b,23-acetate parent nucleus combines with ACE2 amino acid residues LEU85 and HIS15, and hydroxyl and carbonyl groups on the parent nucleus form hydrogen bonds with amino acid residues GLN101 and ASN103. These interactions increase the binding of molecules to proteins.

Table 3 Docking results of the 39 core components with 3CLpro and ACE2

Number	Compound	Binding energy values with 3CLpro(kcal/mol)	Binding energy values with ACE2 (kcal/mol)
1	3'-Methoxyglabridin	-8.3	-6.1
2	Moslosooflavone	-7.8	-6.0
3	Kaempferol	-7.7	-5.9
4	Alisol,b,23-acetate	-7.7	-6.8
5	Quercetin	-7.6	-6.2
6	Peroxyergosterol	-7.6	-5.8

7	Diosmetin	-7.6	-6.3
8	Genkwanin	-7.6	-5.9
9	Epianhydrobelachinal	-7.6	-6.5
10	α-Amyrin	-7.5	-6.7
11	[(1S,3R)-1-[(2R)-3,3-dimethyloxiran-2-yl]-3-[(5R,8S,9S,10S,11S,14R)-11-hydroxy-4,4,8,10,14-pentamethyl-3-oxo-1,2,5,6,7,9,11,12,15,16-decahydrocyclopenta[a]phenanthren-17-yl]butyl] acetate	-7.5	-6.8
12	Areapillin	-7.4	-6.3
13	Naringenin	-7.3	-5.9
14	Glyasperin B	-7.3	-5.7
15	5,8,2'-Trihydroxy-7-methoxyflavone	-7.2	-6.1
16	Galangin	-7.2	-6.0
17	Spinasterol	-7.1	-5.6
18	Cerevisterol	-7.1	-5.6
19	3beta-Hydroxy-24-methylene-8-lanostene-21-oic acid	-7.0	-6.3
20	Poriferast-5-en-3beta-ol	-7.0	-5.5
21	Stigmasterol	-7.0	-5.5
22	beta-sitosterol	-6.9	-6.8
23	Sinensetin	-6.9	-5.5
24	Dehydroeburicoic acid	-6.8	-5.8
25	Alisol B monoacetate	-6.8	-6.0
26	(22e,24r)-ergosta-6-en-3beta,5alpha,6beta-triol	-6.8	-5.5
27	Glypallichalcone	-6.7	-5.4
28	Femara	-6.7	-5.3
29	5,7-dihydroxy-2-(3-hydroxy-4-methoxyphenyl)chroman-4-one	-6.6	-5.5
30	Trametenolic acid	-6.6	-6.4
31	3,5,6,7-tetramethoxy-2-(3,4,5-trimethoxyphenyl)chromone	-6.5	-5.4
32	Sitosterol	-6.5	-5.7
33	Tussilagolactone	-6.5	-4.8
34	Denudatin B	-6.5	-5.4
35	Anhydrobelachinal	--6.5	-5.8
36	(3S,8S,9S,10R,13R,14S,17R)-10,13-dimethyl-17-[(2R,5S)-5-propan-2-yloctan-2-yl]-2,3,4,7,8,9,11,12,14,15,16,17-dodecahydro-1H-cyclopenta[a]phenanthren-3-ol	-6.4	-5.0
37	4,9-dimethoxy-1-vinyl-$b-carboline	-6.3	-5.7
38	Kadsurenone	-6.1	-5.2
39	Gondoic acid	-4.7	-3.9

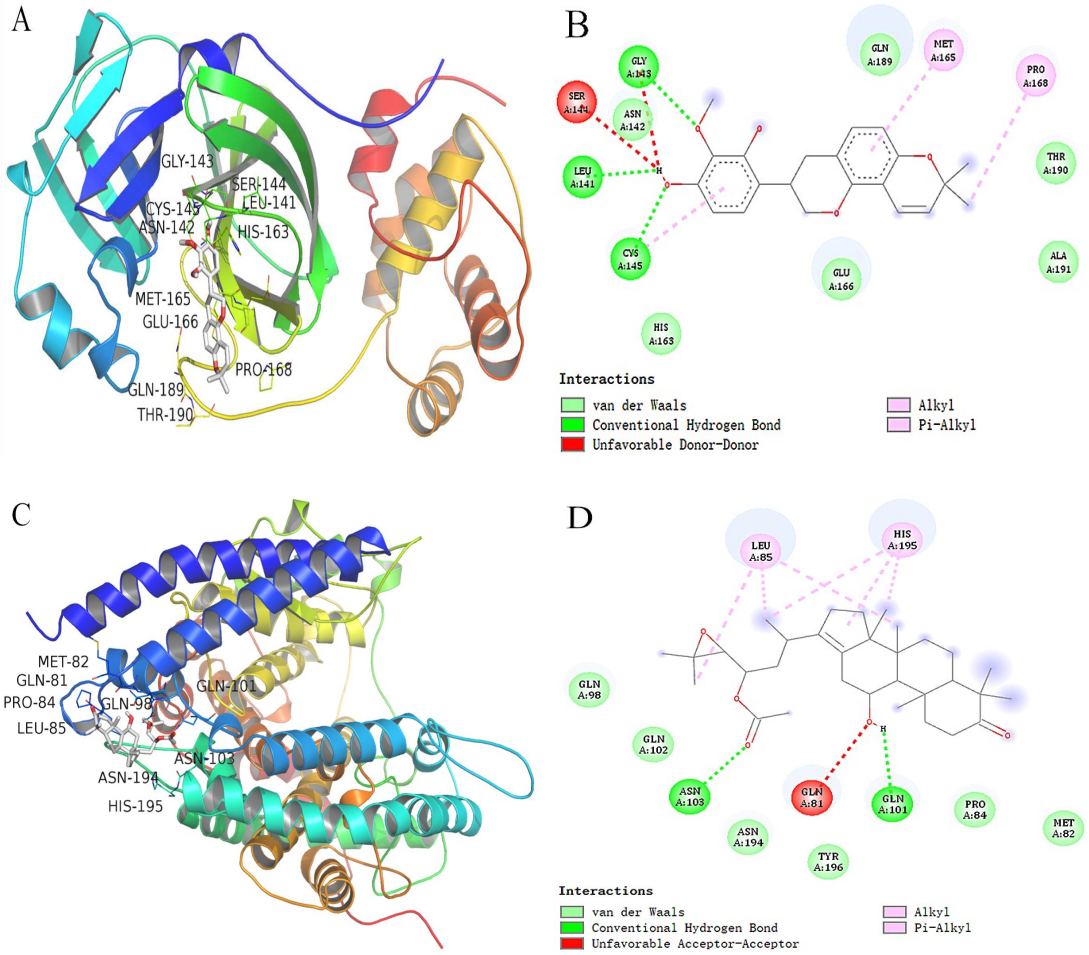

Fig.9 2D and 3D molecular docking diagrams of 3CLpro with 3'-Methoxyglabridin (A, B) and ACE2 with Alisol,b,23-acetate (C, D)

4. Discussion

COVID-19 is a new emergent disease. Although the prevention and treatment methods of COVID-19 have been well studied and achieved good results, there is still a lack of specific drugs, and the variation of SARS-CoV-2 cannot be ruled out.

QFPDD was composed of several classical prescriptions for treating exogenous fever caused by cold evil in the Treatise on Cold Damage and Miscellaneous Diseases written by Zhang Zhongjing in the Han dynasty. The curative effect of this prescription has been clinically tested, and it can effectively relieve symptoms such as fever, cough, and fatigue so that ordinary patients do not develop into severe patients. The positive nucleic acid negative conversion rate is also significantly improved. Therefore, it is highly feasible to find and develop anti-SARS-CoV-2 active

ingredients from this method.

Network pharmacology is based on the overall and systematic interaction of drugs, targets, and diseases, and uses complex network models to express and analyze the pharmacological properties of the research objects [39]. With the research and development of network pharmacology in the field of traditional Chinese medicine, it provides a new perspective and thinking for the systematic study of the complex ingredients of traditional Chinese medicine [40-42]. Therefore, in this study, we constructed and analyzed the target network map of QFPDD and COVID-19, and used these targets for functional enrichment and signal pathway analysis to reveal the potential molecular mechanism of QFPDD in the treatment of COVID-19, and found the main active ingredients and potential target genes of the treatment.

4.1 Main active ingredients

The SARS-CoV-2 isolated from Wuhan is the seventh coronavirus to infect humans discovered so far [43-44]. Rao Zihe/Yang Haitao's research group from Shanghai university of science and technology determined the high-resolution crystal three-dimensional structure of the 2019-nCoV 3CLpro. Previous studies have confirmed that SARS-CoV-2, like SARS-CoV, enters human cells through ACE2 and causes infection [45]. Therefore, the ingredient closely related to the hydrolase and ACE2 of 2019-nCoV 3CLpro will be the main bioactive ingredient of QFPDD against SARS-CoV-2. By this study will be 20 kinds of traditional Chinese medicines (except Gypsum Fibrosum) in QFPDD after the screening of 375 major active ingredients with 3CLpro and ACE2 in molecular docking, the results showed that except taraxanthin and delphinidin, the rest of the ingredients and the two docking binding energy<0, presumably OB $\geqslant$ 30% and DL $\geqslant$ 0.18 ingredients in QFPDD may have direct inhibition of SARS-CoV-2 and inhibition of ACE2 combined with SARS-CoV-2 protein, give play to the role of treatment, for QFPDD became the only a general formula, and became the treatment of this COVID-19 specific drug to provide ample evidence. The 39 core ingredients identified through network pharmacology screening not only have more targets to improve disease symptoms, but

also are most closely related to 3CLpro and ACE2, which may play a major role in the treatment of COVID-19 by QFPDD. Therefore, it is speculated that these 39 ingredients may be the main bioactive ingredients in the treatment of COVID-19 by QFPDD.

4.2 Potential target genes

We found 24 key targets (PIK3CA, PIK3R1, APP, SRC, MAPK1, MAPK3, AKT1, HSP90AA1, EP300, CDK1, JAK2, EGFR, F2, MAPK8, RXRA, ESR1, PRKCD, PTK2, RPS6KB1, MAPK14, NR3C1, PRKCE, CDK5, PPARA) for the treatment of COVID-19. Due to close association, these targets mentioned above are believed to have impacts on COVID-19, which has also been proved by relevant studies. Somatic mutations of the PIK3CA gene are present in many other types of cancer, and these mutations alter individual amino acids in the p110α protein. Mutations in the cancer-related PIK3CA gene lead to changes in p110α, thereby enabling PI3K to signal without regulation, and increased signal transduction can lead to uncontrolled cell proliferation, leading to the development of cancer [46]. The cancer-related changes in the PIK3R1 gene will change the regulatory subunit so that it can no longer control the activity of PI3K, thus significantly increasing PI3K signaling. The increase of PI3K signaling seems to promote the uncontrolled cell growth and division characteristic of cancerous tumors [47]. Amyloid precursor protein (APP) is also considered to be one of the molecules involved in the proliferation and invasion of a variety of human malignant tumor cells, and its phosphorylated form (p-APP) is considered to be an effective prognostic factor for patients with Ad and Sq lung cancer [48]. App42-beta activates mononuclear phagocytes in the brain, causing inflammation and promoting Tau aggregation and TPK II mediated phosphorylation. Laser microdissection neurons extracted from pre-plague APP transgenic rats can produce a variety of effective immune factors at transcription and protein levels [49]. SRC regulates many important mechanisms in both normal and cancer cells and is overexpressed in various tumors, including lung cancer, representing a potential target for cancer treatment [50]. MAPK is considered to be an important regulator of the inflammatory response in ALI. MAPK1 can eliminate LPS induced inflammatory

injury of A549 cells and has a protective effect on lung injury in ALI mice [51]. Abnormal expression of MAPK3 is related to invasion, metastasis, and drug resistance of various tumor cells. Overexpression of mir-129 can inhibit the expression of MAPK3, inhibit cell proliferation, induce cell apoptosis, and reduce cisplatin resistance [52]. The AKT1 gene provides a protein specification for the preparation of AKT1 kinase. The protein is found in all cell types in the body and plays a crucial role in many signaling pathways. AKT1 kinase helps regulate cell growth and division, cell survival, and apoptosis. AKT1 gene belongs to a class of genes called oncogenes, which may cause normal cell canceration after mutation [53-54]. The expression of HSP90AA1 is related to a variety of physiological functions, not only the heat shock response [55]. HSP90AA1 and other genes regulate the pathogenesis of squamous cell lung cancer (SQCLC) caused by chronic obstructive pulmonary disease (COPD). These genes can be used as potential therapeutic targets for the treatment of patients with COPD associated SQCLC [56]. EP300 is a histone acetyltransferase that regulates transcription through chromatin remodeling and plays an important role in cell proliferation and differentiation. EP300 is also a target for viral oncoproteins. Data show that EP300 is mutated in epithelial carcinoma, proving it to be a classic tumor suppressor gene [57]. CDK1 controls the cell cycle, and approximately 75 CDK1 targets have been identified that control key cell cycles such as DNA replication and isolation, transcriptional processes, and cell morphogenesis [58]. JAK2 plays a crucial role in the function of certain types of cytokine receptors [59], and a small-molecule inhibitor of JAK2 is radiosensitizing in lung cancer models [60]. EGFR is more widely expressed in lung cancer tissues than in adjacent normal lungs [61], and pneumonic lung cancer (PLC) has a certain relationship with EGFR gene mutation [62]. F2 plays an important role in protective immunity in fibrin-induced pneumonia and sepsis and enhances platelet-neutrophils interactions [63]. MAPK8 is an important signal molecule in the MAPK signal transduction pathway, and its functions involve various mechanisms such as cell proliferation, cell differentiation, and cell apoptosis [64-65]. RXRA plays a central role in the regulation of many intracellular receptor signaling pathways, and macrophage RXRA plays a key role in the

regulation of innate immunity and has become a potential target for sepsis immunotherapy [66]. ESR1 tumor suppressor gene inactivation occurs in many tumor types, including lung cancer [67]. PKCD is an important regulator of human neutrophil pro-inflammatory signaling and plays an important role in regulating neutrophil-endothelial cell interactions and recruitment in the inflamed lung [68]. Activation of members of the PTK family involved in acute inflammatory responses, such as acute lung injury and sepsis, has been identified as essential for recruitment and activation of monocytes, macrophages, neutrophils, and other immune cells [69]. RPS6KB1 is a member of the ribosomal S6 kinase family that encodes serine/threonine kinases. The encoded protein responds to mTOR (a mammalian target of rapamycin) signaling to promote protein synthesis, cell growth, and cell proliferation. The activity of this gene is associated with human cancer [70]. MAPK14 may play an important role in the development of ventilator-associated pneumonia (VAP) by altering the immune response and MAPK signaling pathway [71]. NR3C1 is involved in the inflammatory response, cell proliferation, and differentiation of target tissues [72]. PRKCE can be used as a breath regulator to participate in mitochondrial respiration, promote the occurrence of mitochondrial organisms, and reduce organ damage caused by pneumonia [73]. CDK5 plays a crucial role in a variety of cancers by regulating the migration and motility of cancer cells [74]. CDK5 gene is overexpressed in non-small cell lung cancer [75]. PPARA plays an important role in lipid metabolism and inflammatory regulation. Previous studies have demonstrated the immune regulatory effect of PPARA and the immunosuppressive effect of PPARA ligand WY14643 on acute lung transplant rejection in rats [76]. According to the results of enrichment analysis, we found that some important targets can regulate a variety of pathways. Among them, MAPK1, MAPK3, PIK3CA, and PIK3R1 participate in more than 90 signaling pathways, reflecting the synergistic effect of multiple targets.

4.3 Functional enrichment and pathway analysis

The enrichment analysis of GO function includes three parts: biological process, molecular function, and cell ingredient [77]. Biological processes include cellular response to nitrogen compound, positive regulation of transferase activity, etc., among

which cellular response to nitrogen compound has the largest enrichment proportion in the biological process. Studies have shown that inhibition of nitric oxide can lead to an increase in the release of pro-inflammatory cytokines, leading to worsening of lung injury. Nitric oxide may have a protective effect on acute lung injury [78]. Molecular functions are mainly concentrated in protein kinase activity, protein tyrosine kinase activity, and kinase binding, among which protein kinase activity has the largest enrichment proportion in molecular functions. Experimental results showed that the mitochondrial antioxidant pathway mediated by protein kinase D1 plays an important role in the early stage of bleomycin-induced pulmonary fibrosis in rats [79]. Similarly, the expression of protein kinase CK2 is related to the prognosis of patients with lung cancer, suggesting that protein kinase CK2 may be a potential target for the treatment of lung cancer, and the inhibition of CK2 kinase activity may be an effective method for the treatment of lung cancer [80]. The cell ingredients are mainly concentrated in the membrane, the receptor complex, and the dendrite, among which the membrane raft has the largest concentration in the cell ingredients. Experiments have shown that lipid raft protein stomatin with low oxygen, and Dex upregulation can stabilize the cytoskeleton connected by the membrane and increase the barrier function of lung epithelial cells, thus having a protective effect on lung tissue cells [81]. According to the enrichment analysis results, we found that the target mainly improved the symptoms of COVID-19 patients through cellular response to nitrogen compound, protein kinase activity, and membrane raft. Therefore, it is speculated that the treatment of COVID-19 by QFPDD may be most closely related to the above pathways.

The KEGG database is a comprehensive database for the systematic analysis of the metabolic pathways of gene products and compounds in cells and the functions of these gene products for functional annotation of the genome or transcriptome of a species. The KEGG pathway analysis showed that Pathways in cancer, Neuroactive ligand-receptor interaction, and PI3K-Akt signaling pathway were significantly more significant in the pathway enrichment analysis, with Pathways in cancer being the most significant. The 24 predicted key targets were most closely related to Pathways

in cancer and Proteoglycans in cancer, indicating that cancer was most closely related to COVID-19. A recent study showed that the COVI-19 infection rate in cancer patients was 0.79%, higher than the overall COVID-19 infection rate in Wuhan on the date of data cut-off, and the risk of COVID-19 infection in cancer patients was 2.31 times that of the general population [82]. Combined with the results of this study, the reasons were analyzed. On the one hand, the immune function of cancer patients was low, during which they were more likely to be infected with the virus. On the other hand, it may be related to key target genes. Most of the 24 potential targets predicted in this study are closely related to cancer [83]. A large amount of experimental evidence indicates that the carcinogenic signal transduction pathway is the basis of the Endocrine resistance, including PI3K-Akt-mTOR，MAPK-ERK，Src，CDK4-CDK6，ER itself and so on. A combination of targeted ER and such pathways is probably the most effective way to combat resistance to antiestrogens, and clinical trials testing such strategies have shown promising results. The PI3K-Akt signaling pathway is involved in the regulation of cellular inflammatory response, stimulating the expression of endothelial nitric oxide synthase (eNOS) and increasing the production of nitric oxide (NO), to increase vascular permeability, promote the infiltration of inflammatory cells, stimulate the activation of inflammatory cells, and secrete a large number of inflammatory factors through the activity of NO [84]. Studies have shown that PI3K inhibitor has A significant inhibitory effect on NO production and inflammatory response in the lung tissues of viral pneumonia mice induced by Influenza A virus (IAV) infection [85]. In this fight against the epidemic, in addition to the remarkable curative effect of Chinese medicine on COVID-19, some western drugs against the virus (HIV or Ebola) have also been found to have a certain curative effect. Through KEGG analysis, we found that these 24 genes are also involved in the transduction of the signaling pathway of Human immunodeficiency virus one infection, which may also be the reason why drugs such as remdesivir, lopinavir/ritonavir, which can fight HIV infection, have some effect on COVID-19.

5. Conclusion

In this study, 39 active ingredients of QFPDD in the treatment of COVID-19 were found through network pharmacology, and 24 potential target genes were identified for the treatment, which was verified by enrichment and pathway analysis to verify the reliability of these ingredients and targets used to evaluate the treatment of COVID-19. Besides, the molecular mechanism of QFPDD in the treatment of COVID-19 was illustrated. According to the results of enrichment analysis, we revealed the synergistic characteristics of multiple targets and found that the targets improved clinical symptoms in COVID-19 patients through cellular response to nitrogen compound, protein kinase activity, and membrane raft. Twenty-four potential target genes are primarily involved in the treatment of COVID-19 by participating in the Pathways in cancer, Endocrine resistance, PI3K-Akt signaling pathway, and Proteoglycans in cancer. This study laid a theoretical foundation for further exploration of QFPDD in the treatment of COVID-19. Although our research has achieved the goal, due to the limitations of network pharmacology, the later research team can carry out experimental research around the material basis-pharmacodynamic evaluation-metabolomics-signaling pathway verification, etc., to provide the experimental basis for the treatment of COVID-19 with QFPDD and the later drug development.

Abbreviations

QFPDD: QingFeiPaiDu Decoction; COVID-19: Corona Virus Disease 2019; SARS-CoV-2: Severe acute respiratory syndrome coronavirus 2; 3CLpro:3-chymotrypsin-like cysteine protease; ACE2: Angiotensin-converting enzyme 2 ; TCMSP: Traditional Chinese Medicine Systems Pharmacology; TCMID: Traditional Chinese Medicines Integrated Database; OB: Oral bioavailability; DL: Drug-likeness; PPI: Protein-protein interaction; GO: Gene Ontology; KEGG: Kyoko Encyclopedia of Genes and Genomes; EH: Ephedrae Herba; GRR: Glycyrrhizae Radix et Rhizoma; ASA: Armeniacae by Amarum; GF: Gypsum Fibrosum; CR:Cinnamomi Ramulus; AR: Alismatis Rhizoma; POL: Polyporus; AMR:

Atractylodis Macrocephalae Rhizoma; POR: Poria; BUP: Bupleuri Radix; SR: Scutellariae Radix; PR: Pinelliae Rhizoma; ZRR: Zingiberis Rhizoma Recens; AST: Asteris Radix et Rhizoma; FF: Farfarae Flos; BR: Belamcandae Rhizoma; ARR: Asari Radix et Rhizoma; DR: Dioscoreae Rhizoma; AFI: Aurantii Fructus Immaturus ; CRP: Citri Reticulatae Pericarpium; PH: Pogostemonis Herba; ASPL: Average shortest path length; BC: Betweenness centrality; CC: Closeness centrality; ALI: Acute lung injury; ARDS: Acute respiratory distress syndrom; APP: Amyloid precursor protein; SQCLC: Squamous cell lung cancer; COPD: Chronic obstructive pulmonary disease; PLC: Pneumonic lung cancer; VAP: Ventilator-associated pneumonia; PKD1: Protein kinase D1; eNOS: endothelial nitric oxide synthase; NO: Nitric oxide; IAV: Influenza A virus.

Acknowledgements

Not applicable.

Authors' contributions

Yan Liu and Lewen Xiong: study concept and design; analysis and interpretation of data; prepared figures; wrote the manuscript text. Yanyu Wang and Mengxiong Luo: acquisition of data. Longfei Zhang and Yongqing Zhang: critical revision of the manuscript for important intellectual content; obtained funding. All authors read and approved the final manuscript.

Funding

This research was funded by the key research and development project of Shandong province: demonstration research on key technologies of precision and industrialization of TCM prescription (2016CYJS08A01)

Availability of data and materials

The datasets used during the current study are available from the corresponding author on reasonable request.

Ethics approval and consent to participate

Not applicable.

Consent for publication

Not applicable.

Competing interests

The authors declare that they have no competing interests.

References

[1] S. J. John, Origins of MERS-CoV, and lessons for 2019-nCoV. The Lancet Planetary Health, (2020), doi:10.1016-S2542-5196(20)30032-2.

[2] V. J. Veljko, Use of the informational spectrum methodology for rapid biological analysis of the novel coronavirus 2019-nCoV: prediction of potential receptor, natural reservoir, tropism and therapeutic/vaccine target. F1000 Research, (2020), doi:10.12688/f1000research. 22149.2.

[3] A. L. Hopkins, Network pharmacology: the next paradigm in drug discovery. Nat Chem Biol, 4 (2008), pp.682-690.

[4] J. L. Ru, P. Li, J. N. Wang, et al., TCMSP: a database of systems pharmacology for drug discovery from herbal medicines. Journal of Cheminformatics, 6(2014), p.13.

[5] R. Xue, Z. Fang, M. Zhang, et al., TCMID: traditional Chinese medicine integrative database for herb molecular mechanism analysis. Nucleic Acids Res, 41(2013), pp.1089-1095.

[6] S. S. Ahmed, V. Ramakrishnan, Systems biological approach of molecular descriptors connectivity: Optimal descriptors for oral bioavailability prediction. PLoS

One, 7(2012), p.40654.

[7] O. Ursu, A. Rayan, A. Goldblum, et al., Understanding drug-likeness. Wires Comput Mol Sci, 1(2011), pp.760-781.

[8] E. E. Bolton, J. Chen, S. Kim, et al., PubChem3D: a new resource for scientists. J Cheminform 3(2011), p.32.

[9] A. Daina, O. Michielin, V. Zoete, SwissTargetPrediction: updated data and new features for efficient prediction of protein targets of small molecules. Nucleic Acids Res, 47(2019), pp.357-364.

[10] P. Shannon, A. Markiel, O. Ozier, et al., Cytoscape: a software environment for integrated models of biomolecular interaction networks. Genome Res, 13(2003), pp.2498-2504.

[11] M. E. Smoot, K. Ono, J. Ruscheinski, et al., Cytoscape 2.8: new features for data integration and network visualization. Bioinformatics, 27(2011), pp.431-432.

[12] X. X. Xu, R. Li, J. Chen, Prediction of anti-pancreatic cancer targets and molecular mechanism of resveratrol based on network pharmacology, Journal of sichuan physiological sciences, 41(2019), pp.1-4.

[13] S. Fishilevich, S. Zimmerman, A. Kohn, et al., Genic insights from integrated human proteomics in GeneCards. Database (Oxford), 2016(2016), pp.1-17.

[14] H. Yang, C. Qin, Y. H. Li, et al., Therapeutic target database update 2016: enriched resource for bench to clinical drug target and targeted pathway information. Nucleic Acids Res, 44(2015), pp.1069-1074.

[15] D. S. Wishart, C. Knox, A.C. Guo, et al., DrugBank: a comprehensive resource for in silico drug discovery and exploration. Nucleic Acids Res, 34(2006), pp.668-672.

[16] J. Piñero, N. Queralt-Rosinach, À. Bravo, et al. DisGeNET: a discovery platform for the dynamical exploration of human diseases and their genes. Database (Oxford), 15(2015), pp.1-17.

[17] A. Hamosh, A. F. Scott, J. S. Amberger, et al., Online Mendelian Inheritance in Man (OMIM), a knowledgebase of human genes and genetic disorders. Nucleic Acids Res, 33(2005), pp.514-517.

[18] P. Shannon, A. Markiel, O. Ozier, et al., Cytoscape: a software environment for integrated models of biomolecular interaction networks. Genome Res, 13(2003), pp.2498-2504.

[19] C. Von Mering, L. J. Jensen, B. Snel, et al., STRING: known and predicted protein-protein associations, integrated and transferred across organisms. Nucleic Acids Res, 33(2005), pp.433-437.

[20] D. Szklarczyk, A. Franceschini, S. Wyder, et al., STRING v10: protein-protein interaction networks, integrated over the tree of life. Nucleic Acids Res, 43(2015), pp.447-452

[21] D. Szklarczyk, J. H. Morris, H. Cook, et al., The STRING database in 2017: quality-controlled protein–protein association networks, made broadly accessible. Nucleic Acids Res, 45(2017), pp.362-368.

[22] Y. Zhou, B. Zhou, L. Pache, et al., Metascape provides a biologist-oriented resource for the analysis of systems-level datasets. Nat Commun, 10(2019), p.1523.

[23] D. W. Huang, B. T. Sherman, R. A. Lempicki, Systematic and integrative analysis of large gene lists using DAVID bioinformatics resources. Nat Protoc, 4(2008), pp.44-57.

[24] M. Kanehisa, S. Goto, KEGG: kyoto encyclopedia of genes and genomes. Nucleic Acids Res, 28(2000), pp.27-30.

[25] H. Ogata, S. Goto, K. Sato, Fujibuchi W., Bono H., Kanehisa M., KEGG: Kyoto Encyclopedia of Genes and Genomes. Nucleic Acids Res, 27(1999), pp.29-34.

[26] Z. P. Li, H. J. Chen, S.H. Chang, et al., Changes in Th17/Treg cell balance and the role of Notch signaling pathway in mycoplasma pneumonia in children. Journal of Chinese hospital infectiology, 7(2020), pp.1048-1052.

[27] R. Q. Duan, C. Q. Li, Effect of azithromycin combined with montelukast sodium on NOD-like receptor protein-3 pathway in children with mycoplasma pneumoniae pneumonia. China medical engineering, 27(2019), pp.90-92.

[28] H. Tan, H. Ji, N. Li, et al., Relationship between TGF-β and ERK/GSK3β activation of signaling pathway and radiation-induced mesenchymal transformation of alveolar epithelial cells in rats with radiation-induced pneumonia. Journal of Guangxi

medical university, 36(2019), pp.1909-1914.

[29] J. J. Xue, X. X. Shi, Expression of TLRs in peripheral blood mononuclear cells of children with mycoplasma pneumonia and its effect on NF-κB/IκBα pathway. Chinese journal of health laboratory sciences, 29(2019), pp.2433-2436.

[30] T. T. Wang, C. H. Leng, K. P. Guo, et al., Effect of quercetin on the prevention and treatment of staphylococcus aureus pneumonia in mice and the mechanism of IKK/NF-κB/IκB signaling pathway. Chinese medicine pharmacology and clinic, 35(2019), pp.53-57.

[31] X. K. Wang, Experimental study on prevention and treatment of radioactive pneumonia by regulating AMPK mediated autophagy by qingfei yiyin prescription. Beijing: China academy of Chinese medical sciences, 2019.

[32] Z. M. Liu, Y. Sun, Y. C. Gao, et al., Reduction of inflammatory response in aged klebsiella pneumoniae rats by nomilin inhibition of the TLR4/NF-κB inflammatory pathway. Chinese journal of immunology, 35(2019), pp.970-975.

[33] P. Huang, Y. H. Guo, X. L. Xu, et al., The role of PI3K/Akt/mTOR signaling pathway in the regulation of Treg/Th17 balance in severe pneumonia and the research progress of traditional Chinese medicine. Chinese acute medicine, 27(2018), pp.2245-2247.

[34] Y. X. Huang, Effect of rhIFN-α1b on RSV infection in rats and the signaling pathways of JAK/STAT and TLR4/NF-κB. Xi 'an: fourth military medical university, 2015.

[35] G. M. Hui, Effect of qingfei peiyuan granule on IL-17 and JAK-STAT signaling pathways in BALB/c mouse model of immunocompromised lung infection. Henan: Henan university of traditional Chinese medicine, 2014.

[36] X. Mei, Effects of toxin clearance on JAK/STAT signal transduction pathway in lung tissue of rats with phlegm-heat syndrome of pneumonia. Henan: Henan university of traditional Chinese medicine, 2010.

[37] X. K. Guo, Study on the role of HIF-1α in the regulation of inflammatory factors by nuclear translocation in severe pneumonia caused by influenza a (H1N1) virus infection. Shanghai: Shanghai jiao tong university, 2017.

[38] X. F. Wang, S. Y. Chen, F.Chen, Research progress on the role of Epac/Rap1 signaling pathway in acute lung injury. Chinese journal of pharmacology and toxicology, 26(2012), pp.680-683.

[39] W. X. Zhou, X. R. Cheng, Y. X. Zhang, Network pharmacology: a new concept of drug discovery and understanding. Chinese journal of pharmacology and toxicology, 26(2012), pp.4-9.

[40] W. J. Zhang, Y. H. Wang, Network pharmacology: new ideas for understanding and discovering drugs, World Chinese medicine, 10(2015), pp.280-286.

[41] Y. Q. Zhang, S. Li, Some advances in network pharmacology and modern research of traditional Chinese medicine. Chinese journal of pharmacology and toxicology, 29(2015), pp.883-892.

[42] Y. H. Wang, L. Yang, Research system of modern Chinese medicine based on systematic pharmacology. World Chinese medicine, 8(2013), pp.801-808.

[43] J. Y. Chen, J. S. Shi, D. A. Qiu, et al., Wuhan 2019 coronavirus genome bioinformatics analysis. Bioinformatics, 2020.

[44] C. L. Xiong, L. F. Jiang, Q. W. Jiang, Epidemic and control of human disease caused by ling-coronavirus. Shanghai journal of preventive medicine, 32(2020), pp.1-12.

[45] P. Zhou, X. L. Yang, X. G. Wang, et al., A pneumonia outbreak associated with a new coronavirus of probable bat origin. Nature, 579(2020), pp.270-273.

[46] ML. Filipenko, NA. Os'kina, IA. Oskorbin, et al., Association between the Prevalence of Somatic Mutations in PIK3CA Gene in Tumors and Clinical and Morphological Characteristics of Breast Cancer Patients. Bull Exp Biol Med. 163(2017), pp.250-254.

[47] J. Munkley, K. E. Livermore, U. L. McClurg, et al., The PI3K regulatory subunit gene PIK3R1 is under direct control of androgens and repressed in prostate cancer cells. Oncoscience. 2(2015), pp.755-64.

[48] S. Ito, Y. Miki, R. Saito, et al., Amyloid precursor protein and its phosphorylated form in non-small cell lung carcinoma. Pathol. Res. Pract. 215(2019), p.152463.

[49] L. A. Welikovitch, S. Do Carmo, Z. Maglóczky, et al., Early intraneuronal amyloid triggers neuron-derived inflammatory signaling in APP transgenic rats and human brain. Proc. Natl. Acad. Sci. U.S.A. 117(2020), pp.6844-6854.

[50] D. Lee, O. Gautschi, Clinical development of SRC tyrosine kinase inhibitors in lung cancer.Clin Lung Cancer. 7(2006), pp.381-384.

[51] S. Zhu, W. Song, Y. Sun, et al., MiR-342 attenuates lipopolysaccharide-induced acute lung injury via inhibiting MAPK1 expression. Clin Exp Pharmacol Physiol. 2020, pp.1440-1681.

[52] H. Y. Cao, C. H. Xiao, H. J. Lu, et al., MiR-129 reduces CDDP resistance in gastric cancer cells by inhibiting MAPK3. Eur Rev Med Pharmacol Sci, 23(2019), pp.6478-6485.

[53] J. Wang, Study on Akt1 phosphorylated nuclear matrix binding protein SATB1 and its functions. Shandong, shandong university, 2010.

[54] L. Shen, Preliminary study on the biological function of Akt protein kinase. Xi 'an, fourth military medical university, 2005.

[55] A. D. Zuehlke, K. Beebe, L. Neckers, et al., Regulation and function of the human HSP90AA1 gene. Gene. 570(2015), pp.8-16.

[56] L. Wang, H. Zhao, L. Zhang, et al., HSP90AA1, ADRB2, TBL1XR1 and HSPB1 are chronic obstructive pulmonary disease-related genes that facilitate squamous cell lung cancer progression. Oncol Lett. 19(2020), pp.2115-2122.

[57] S. A. Gayther, S. J. Batley, L. Linger, Mutations truncating the EP300 acetylase in human cancers. Nat Genet. 24(2000), pp.300-303.

[58] J. M. Enserink, R. D. Kolodner, An overview of Cdk1-controlled targets and processes. Cell Div. 2010, p.11

[59] E. Parganas, D. Wang, D. Stravopodis, et al., Jak2 is essential for signaling through a variety of cytokine receptors. Cell. 93(1998), pp.385-395.

[60] Y. Sun, L. Moretti, N. J. Giacalone, et al., Inhibition of JAK2 signaling by TG101209 enhances radiotherapy in lung cancer models. J Thorac Oncol. 6(2011), pp.699-706.

[61] J. G. Paez, P. A. Jänne, J. C. Lee, et al., EGFR mutations in lung cancer:

correlation with clinical response to gefitinib therapy. Science. 304(2004), pp.1497-500.

[62] A. Taus, F. Zuccarino, C. Trampal, et al., EGFR-Mutant Lung Adenocarcinoma Mimicking a Pneumonia. Case Rep Pulmonol. 2012;2012:257827.

[63] T. A. Claushuis, S. F. Stoppelaar, I. Stroo, et al., Thrombin contributes to protective immunity in pneumonia-derived sepsis via fibrin polymerization and platelet-neutrophil interactions. J Thromb Haemost. 15(2017), pp.744-757.

[64] S. W. Kim, A. M. Muise, P. J. Lyons, et al., Regulation of adipogenesis by a tran-scriptional repressor that modulates MAPK activation. J Biol Chem, 276(2001), pp.10199-10206.

[65] C. Tournier, P. Hess, D. D Yang, et al., Requirement of JNK for stress-induced activation of the cytochrome c-mediated death pathway. Sci-ence, 288(2000), pp.870-874.

[66] V. Núñez, D. Alameda, D. Rico, et al., Retinoid X receptor alpha controls innate inflammatory responses through the up-regulation of chemokine expression. Proc Natl Acad Sci U S A. 107(2010), pp.10626-31.

[67] Y. Suga, K. Miyajima, T. Oikawa, et al., Quantitative p16 and ESR1 methylation in the peripheral blood of patients with non-small cell lung cancer. Oncol Rep. 20(2008), pp.1137-1142.

[68] M. J. Mondrinos, T. Zhang, S. Sun, et al., Pulmonary endothelial protein kinase C-delta (PKCδ) regulates neutrophil migration in acute lung inflammation. Am J Pathol. 184(2014), pp.200-213.

[69] D. Okutani, Src protein tyrosine kinase family and acute lung injury. Nihon Rinsho Meneki Gakkai Kaishi. 29(2006), pp.334-341.

[70] National Center for Biotechnology Information. PubChem Database. NCBI Gene=6198, https://pubchem.ncbi.nlm.nih.gov/gene/RPS6KB1/human (accessed on Apr. 10, 2020)

[71] X. Xu, B. Yuan, Q. Liang, et al., Gene expression profile analysis of ventilator-associated pneumonia. Mol Med Rep. 12(2015), pp.7455-7462.

[72] National Center for Biotechnology Information. PubChem Database. NCBI

Gene=2908, https://pubchem.ncbi.nlm.nih.gov/gene/NR3C1/human (accessed on Apr. 10, 2020)

[73] H. Aslami, W. P. Pulskens, M. T. Kuipers, et al., Hydrogen sulfide donor NaHS reduces organ injury in a rat model of pneumococcal pneumosepsis, associated with improved bio-energetic status. PLoS One. 8(2013), p.63497.

[74] K. Wei, Z. Ye, Z. Li, et al., An immunohistochemical study of cyclin-dependent kinase 5 (CDK5) expression in non-small cell lung cancer (NSCLC) and small cell lung cancer (SCLC): a possible prognostic biomarker. World J Surg Oncol. 14(2016), p.34.

[75] H. S. Choi, Y. Lee, K. H. Park, et al., Single-nucleotide polymorphisms in the promoter of the CDK5 gene and lung cancer risk in a Korean population. J Hum Genet. 54(2009), pp.298-303.

[76] J. Yanagisawa, T. Shiraishi, A. Iwasaki, et al., PPARalpha ligand WY14643 reduced acute rejection after rat lung transplantation with the upregulation of IL-4, IL-10 and TGFbeta mRNA expression. J Heart Lung Transplant. 28(2009), pp.1172-1179.

[77] X. Wang, T.S. Yin, B.Y. Li, et al., Progress of gene function enrichment analysis. Chinese science: life science, 46(2016), pp.363-373.

[78] H.B. Qiu, D.C. Chen, J.Q. Pan, et al., Regulatory effect of inhibition of nitric oxide synthesis on inflammatory response in acute lung injury. Emergency medicine, 3(1999), pp.153-155.

[79] N. Ni, N.G. Liu, H.Y. Gao, et al., Effect of active vitamin D3 on d1-mediated antioxidant pathway in rat pulmonary fibrosis. Journal of anatomy, 39(2016), pp.534-538.

[80] Q. W. Li, Study on enhanced radiosensitivity of non-small cell lung cancer by inhibiting protein kinase CK2 activity and its mechanism. Hubei: Huazhong university of science and technology, 2018.

[81] J. Lu, J.C. Chen, H.Y. Cai, et al., Expression of lipidin stomatin in rat lung and A549 cells induced by hypoxia or/and glucocorticoid and its effect on cytoskeleton. Chinese journal of pathophysiology, 26(2010), p.2072.

[82] J. Yu, W. Ouyang, M. L. K. Chua, et al., SARS-CoV-2 Transmission in Patients with Cancer at a Tertiary Care Hospital in Wuhan, China. JAMA Oncol. 2020 Mar 25.

[83] T. W. Miller, Endocrine resistance: what do we know? Am Soc Clin Oncol Educ Book 2013.

[84] X. L. Yin, J. Y. Zhang, W. D. Liu, et al., Inhibition of influenza a virus-induced viral pneumonia by the PI3K/AKT/eNOS pathway mediated by 1-phosphospingosinol receptor 2. Chinese journal of pathophysiology, 34(2008), pp.2062-2067.

[85] Y. L. Yang, M. L. Tu, M. S. Xie, Effects of PI3K inhibitor on NO production and inflammatory response in lung tissues of viral pneumonia mice induced by influenza a virus FM1 infection. Acta virosinica, 35(2019), pp.713-720.

Figures

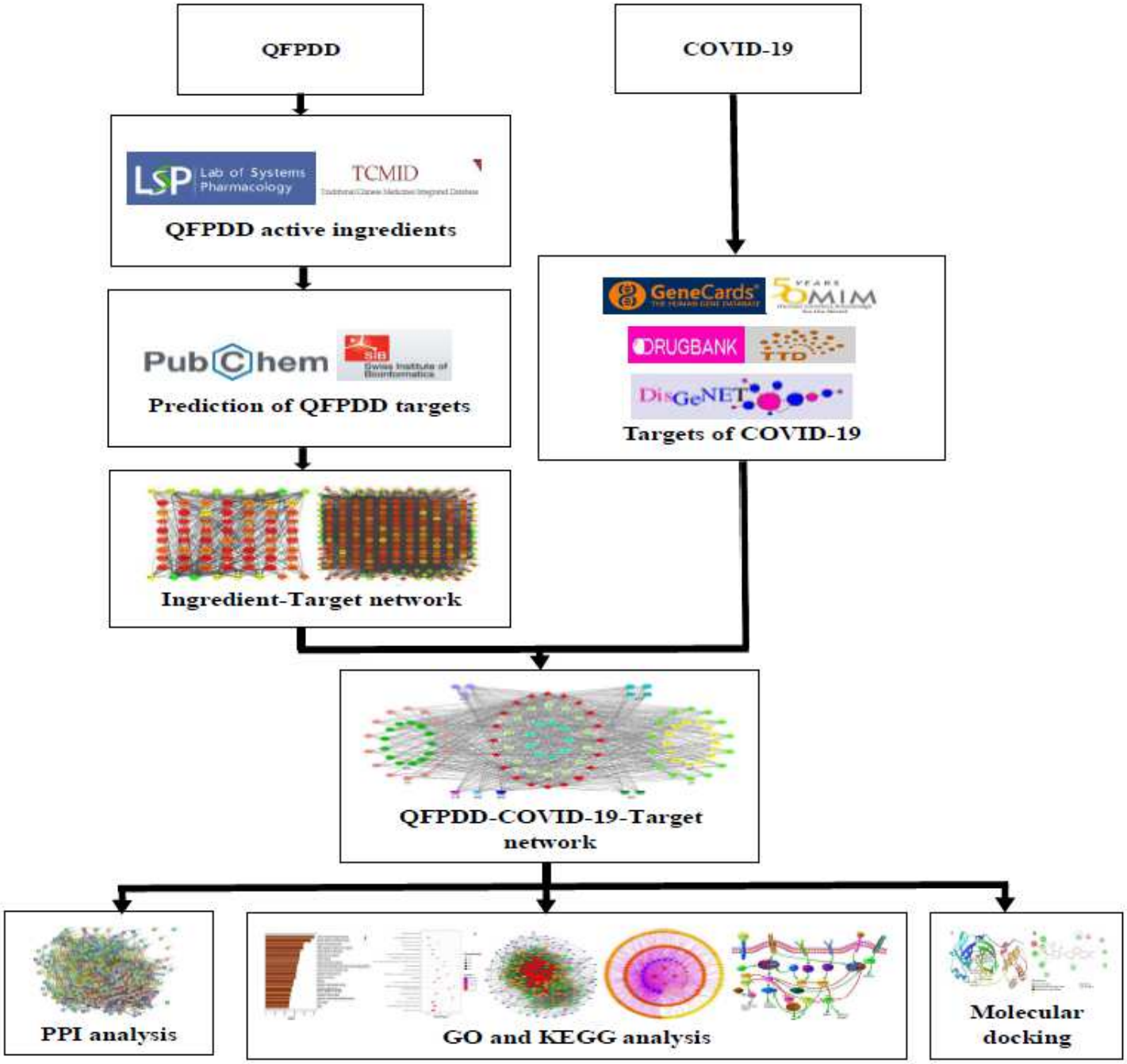

Figure 1

The workflow diagram of QFPDD in the treatment of COVID-19

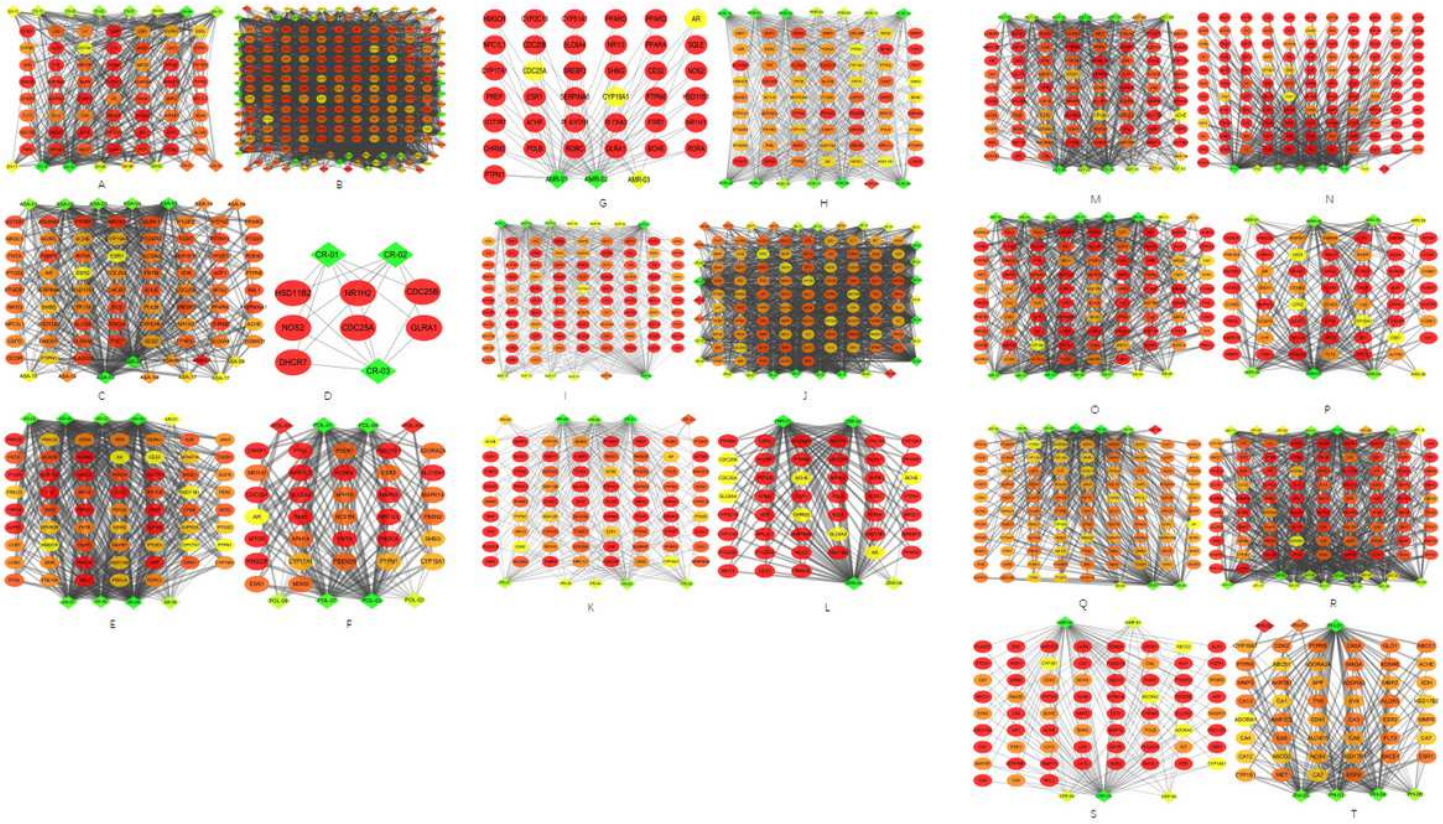

Figure 2

Ingredient-Target network (A)EH□(B)GRR□(C)ASA□(D)CR□(E)AR□(F)POL□(G)AMR,(H)POR,(I)BUP□ (J)SR□ (K)PR□(L)ZRR□(M)AST□(N)FF□(O)BR□(P)ARR□(Q)DR□(R)AFI□ (S)CRP□(T)PH (The rhomboid node represents the ingredient, and the circular node represents the target. The color of the node is represented in ascending order of degrees of freedom from red to yellow to green, and the size of Edge betweenness denotes the thickness of the line.)

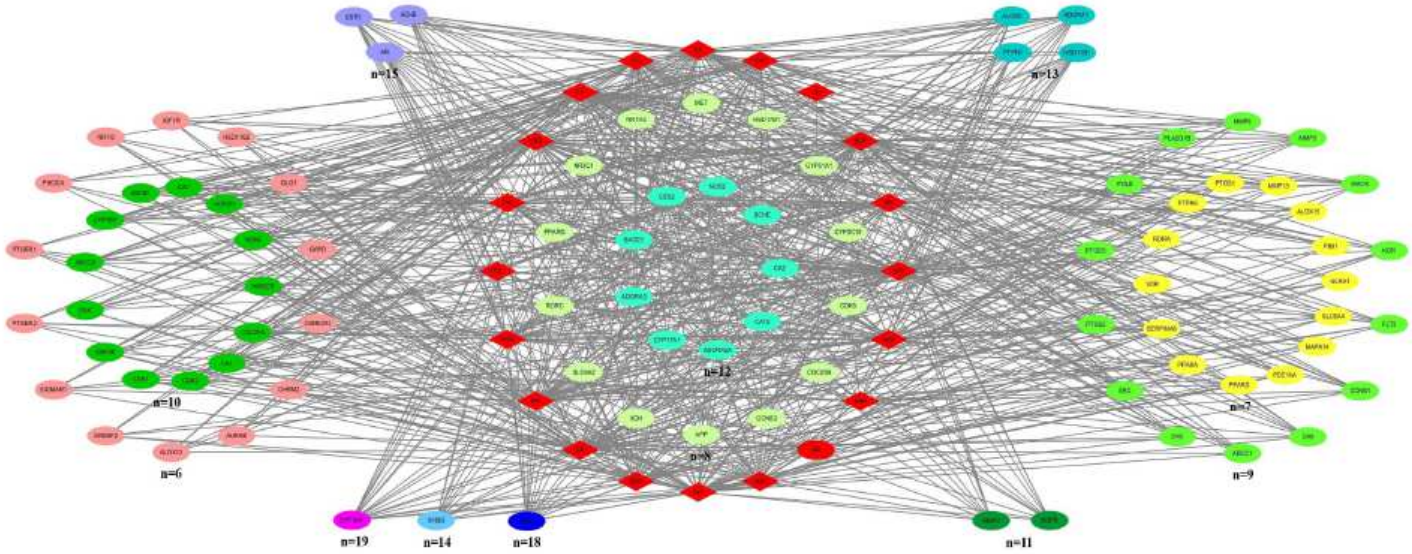

Figure 3

QFPDD-COVID-19-Target Network

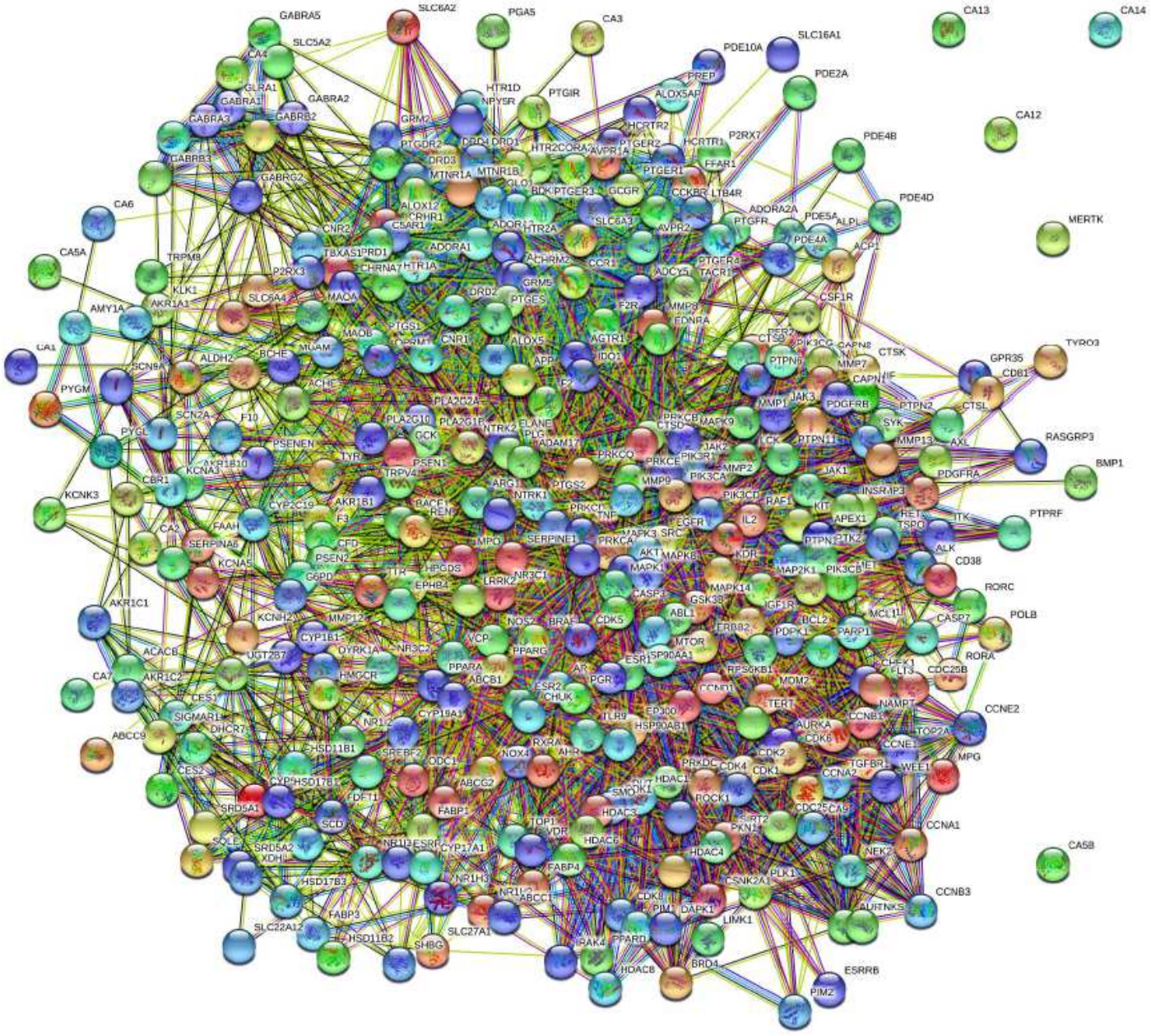

Figure 4

Protein-protein interaction (PPI) network of potential targets of COVID-19 treated with QFPDD

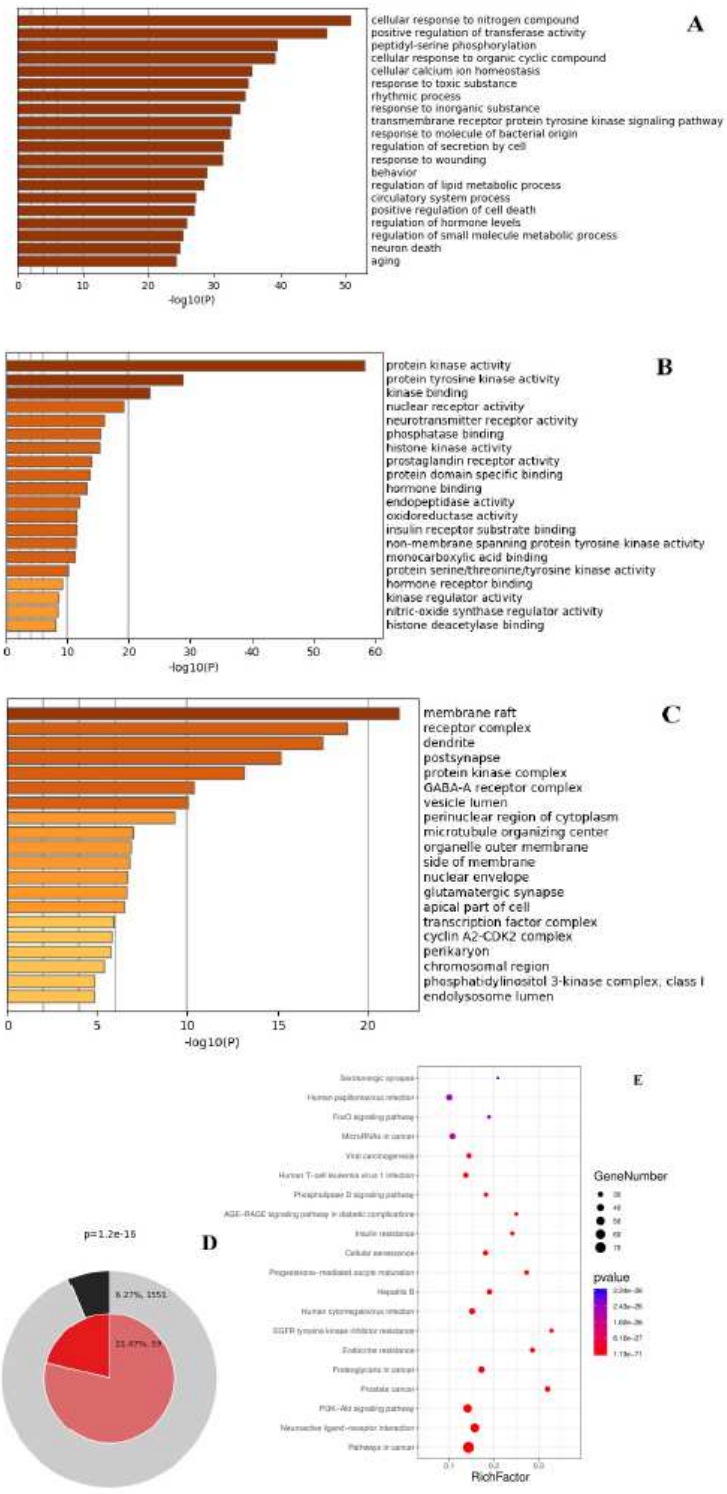

Figure 5

GO enrichment analysis and KEGG pathway analysis of potential targets in QFPDD (A) Enrichment analysis of biological processes (B) Enrichment analysis of molecular functions (C) Enrichment analysis of cell ingredients. The bars of each enrichment item were colored with p values. (D) Biological process enrichment of genes matching membership term: lung. The outer pie shows the number and the percentage of genes in the background that is associated with the membership (in black); the inner pie

shows the number and the percentage of genes in the individual input gene list that is associated with the membership. The p-value indicates whether the membership is statistically significantly enriched in the list. (E) KEGG pathway analysis. The size of the bubble in the figure represents the gene count of this line, and the color from cold to hot represents the P-value from large to small. Fig.

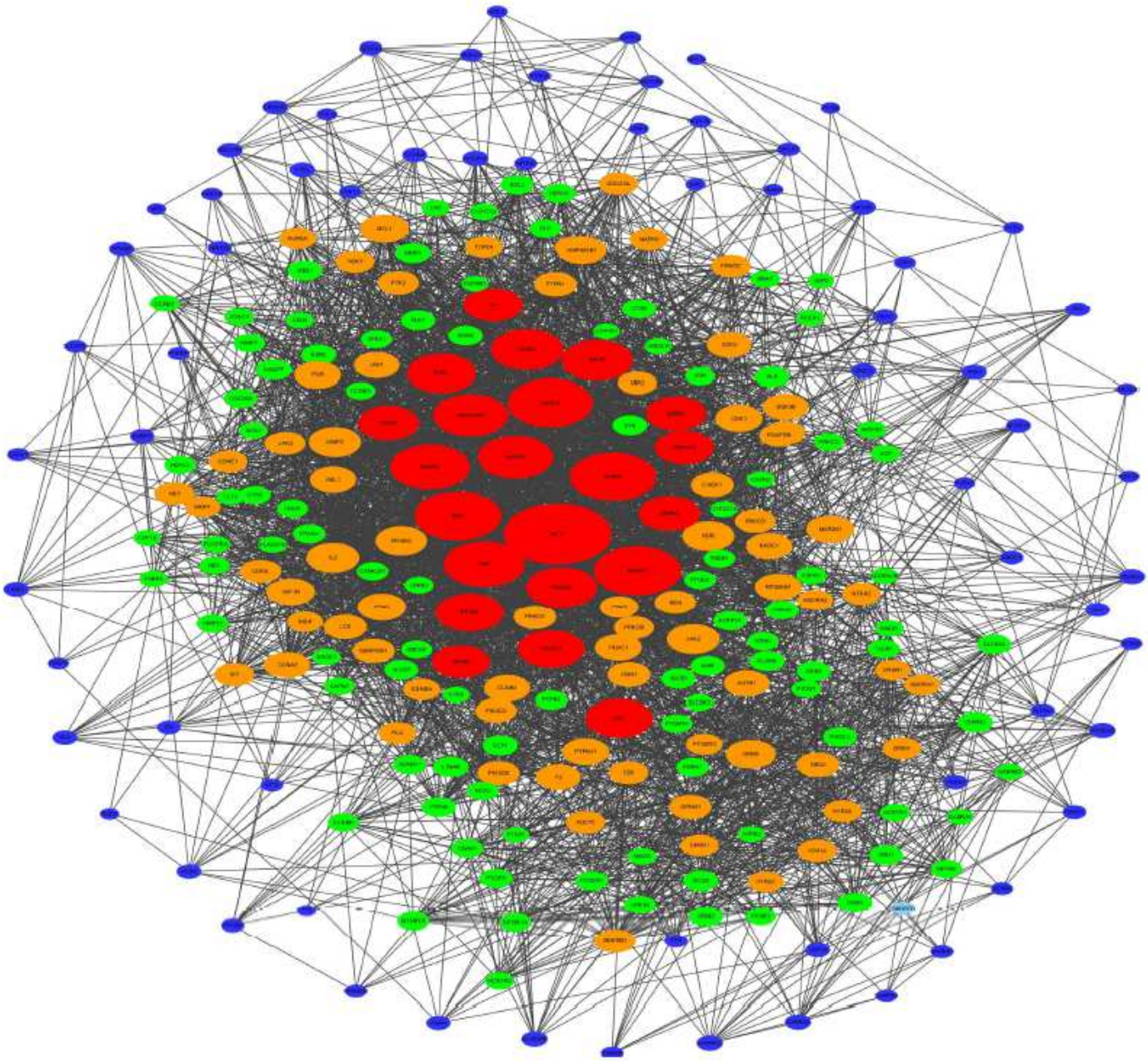

Figure 6

Gene associations on different signaling pathways (the size of nodes in the figure represents the size of degree)

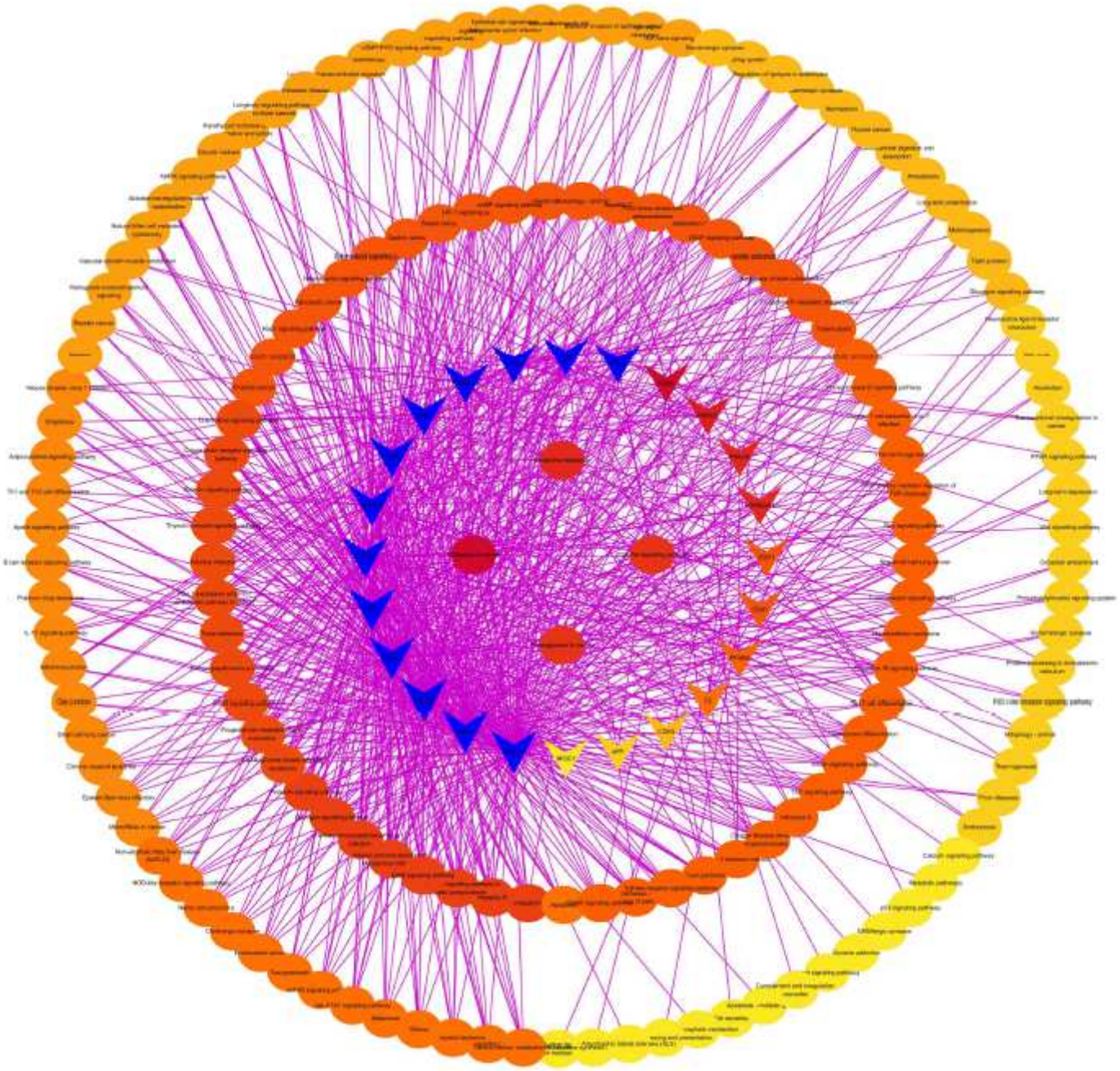

Figure 7

Target-Signal pathway diagram (the circular node represents the signal pathway in which 24 key targets participate, and the v-shaped node represents 24 key targets. The color of the node is represented by ascending order of degree from yellow to orange to red to blue)

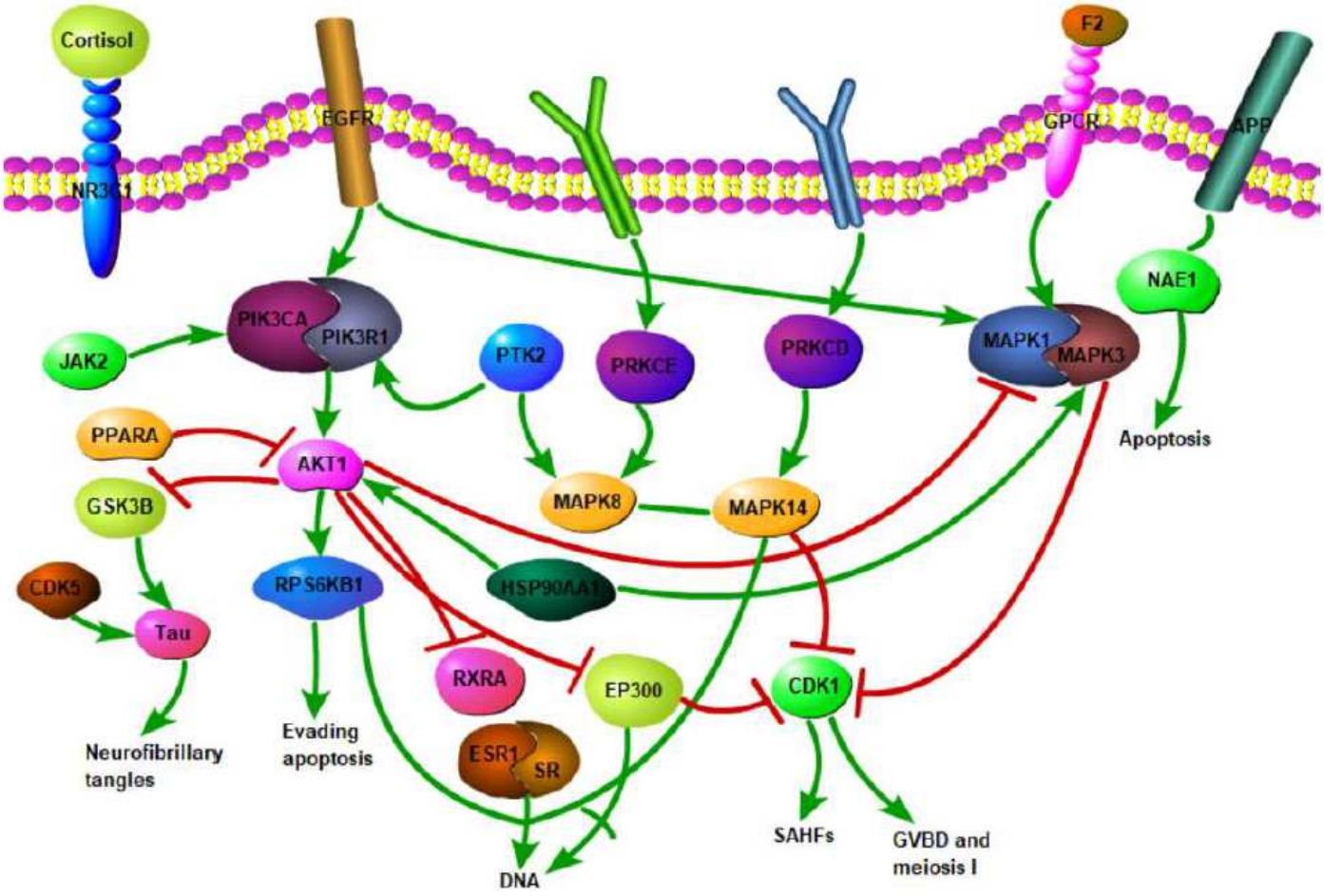

Figure 8

Schematic diagram of 24 critical targets involved in the treatment of COVID-19 signaling pathway (all targets are expressed by gene name)

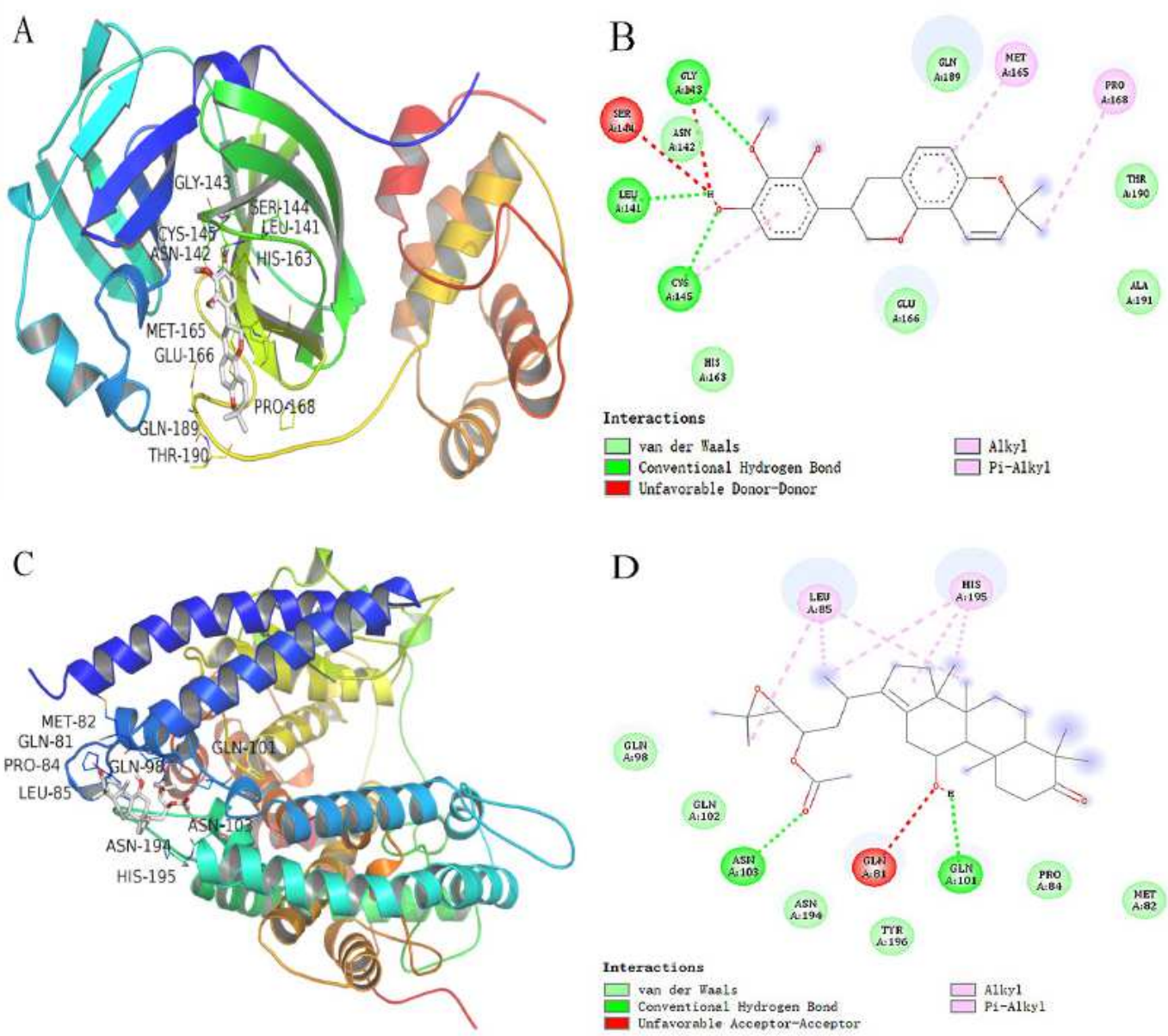

Figure 9

2D and 3D molecular docking diagrams of 3CLpro with 3'-Methoxyglabridin (A, B) and ACE2 with Alisol,b,23-acetate (C, D)

Supplementary Files

This is a list of supplementary files associated with this preprint. Click to download.

- Supplementaryfile1.xlsx
- Supplementaryfile1.xlsx
- Supplementaryfile2.xlsx

- Supplementaryfile2.xlsx